

# Obtaining CBED Patterns

## CHAPTER PREVIEW

We know that SAD, while giving us useful information about the specimen, has two severe limitations.

- We have to be very cautious in interpreting SADPs from areas which are  $< \sim 0.5 \mu\text{m}$  in diameter because the information in the pattern may not be limited to that region. This scale is still large compared to the dimensions of many crystalline features that interest us in materials science and much larger than nanotechnology dimensions.
- SADPs contain only rather imprecise 2D crystallographic information because the Bragg conditions are relaxed for thin specimens and small grains within the specimen (see Chapter 17).

The technique of CBED overcomes both of these limitations and also generates much new diffraction information which we will introduce to you in Chapter 21 and expand in greater depth in the companion text.

In this chapter, we will show you how simple it is to use the versatility of modern TEMs to create a range of CBED patterns containing a variety of very useful contrast effects such as higher-order Laue-zone (HOLZ) spots and lines. In Chapter 21 and the companion text, you will see why these HOLZ features are so useful. They can give us a complete 3D crystallographic analysis of our specimens. By now you are well aware that a major advantage of doing anything in TEM is that we can get the information at high spatial resolution at the same time as we are looking at the TEM image. CBED is no exception. For most TEM operations, thinner specimens are better, but CBED patterns, like Kikuchi patterns, are generally more useful from thicker specimens in which dynamical scattering is occurring. Finally, as with many other sophisticated analytical techniques, CBED uses various obscure initials and acronyms which we will attempt to clarify as we introduce them.

### 20.1 WHY USE A CONVERGENT BEAM?

Historically, CBED is the oldest electron-diffraction technique used in the TEM. It was originally developed by Kossel and Möllenstedt, well before LePoole developed SAD. While SAD is the classic way to relate the diffraction-contrast information in the TEM image to the specimen orientation, it has a notable disadvantage. Remember, we saw back in Chapters 9 and 11 that the diameter of the smallest area you can select by SAD is  $\sim 0.5 \mu\text{m}$ , with an uncertainty of similar dimensions. However, if you have an intermediate-voltage HRTEM with a very low  $C_s$  you may be able to extend the range of SAD to analyze areas  $\sim 100 \text{ nm}$  in diameter, which is still too large for examining any nanoscale material

(particles, films, devices) as well as all crystal defects and most second-phase precipitates which influence the properties of conventional engineering materials. All these features are much smaller than  $0.1 \mu\text{m}$ . As we described back in Figure 9.4, one way we can overcome this limitation is to use a convergent beam of electrons. The region sampled by the convergent beam is a function of its size and the beam-specimen interaction volume, which increases with specimen thickness but is generally a lot smaller than the spatial limitations of SAD. In fact, several so-called micro- and nanodiffraction methods have been developed over the past 40 years to overcome the spatial-resolution limitations of SAD in a TEM. But CBED is by far the most simple and versatile of these techniques and easily

penetrates the nanotechnology domain ( $< 100$  nm), in fact all the way down to single unit-cell dimensions (truly nanodiffraction).

In addition to offering improved spatial resolution, CBED patterns contain a wealth of crystallographic and other data which are difficult or impossible to obtain via SAD and we'll describe much of this new information in the next chapter and in the companion text.

With such capabilities, CBED has transformed diffraction in the TEM from the 'poor relative' of X-ray and neutron diffraction to a more versatile and, in some senses, a unique technique. CBED has already begun to intrude significantly into XRD's traditional domain of quantitative crystallography, as a cursory reading of the contents of *Acta Crystallographica* will show.

Some would argue persuasively that CBED should be the diffraction method of first choice when operating a TEM and this is not surprising given all the new information you can access via CBED. However, much of diffraction theory, indexing methods, etc., were historically developed for parallel-beam SADPs, and standard BF/CDF and other imaging techniques build on such patterns. So we have chosen to construct the text starting with SAD and treat CBED as an 'enriched' variant of SAD.

### THE CBED ADVANTAGE

...over all other diffraction techniques is that most of the information is generated from minuscule regions beyond the reach of other diffraction methods.

In this chapter, we will concentrate on how you can control the experimental variables to acquire and index CBED patterns. In the next chapter, we will introduce to you, among other things, how to perform the basics of what is known as 'electron crystallography.' All the advantages of CBED can simultaneously be coupled with TEM images and spectrometry data thus allowing you to achieve a remarkable degree of characterization of the same region of your specimen at the same time.

There are two potential drawbacks which you should always keep in mind

- The focused probe may generate contamination which can cause localized stresses.
- The convergent beam may heat or damage the chosen region of your specimen.

In early probe-forming TEMs, the operator only had a few seconds to observe and record the CBED pattern before carbon contamination built up to a thickness which masked all the information. Modern TEMs, particularly UHV instruments, should not suffer from this problem (see Chapter 8). You should be able to study small regions of a clean specimen for many minutes or even hours without contamination.

### CONTAMINATION

Most contamination is caused by the specimen-preparation process or your careless handling of your specimen.

As we described in Chapter 4, beam heating/damage may be a problem in materials with poor thermal conductivity but this can be minimized by applying a thin conductive coating or, preferably, by using a liquid-N<sub>2</sub> cooling holder. This latter approach has other advantages for CBED, as we'll see.

You will probably find that it is experimentally easier to do CBED rather than SAD. SAD is used if your primary interest is the image. In CBED, there's no inserting and removing of diaphragms and more information is almost always obtained, invariably from smaller regions. You might not find this fact reflected in your reading of the TEM literature, but remember that researchers (including the authors) often use the technique with which they are most familiar, rather than the best one available. It's also appropriate here to mention why we include the 'E' in CBED but rarely in SAD; it's only so we can pronounce the initials as "see-bed." (Happily no one ever says "sad" or "said" for that matter.) But if the world were logical then all men would ride sidesaddle.

### THE CBED HOLDER

A double-tilt, cooling, low-background holder is really useful for CBED.

## 20.2 OBTAINING CBED PATTERNS

*First, which holder should you use?* As with SAD you will need to do a lot of tilting so a double-tilt holder is required. Some of the diffraction phenomena we will be describing become more visible if the specimen is cooled to liquid-N<sub>2</sub> temperatures. If you want to carry out XEDS and CBED simultaneously then you'll also need a low-background holder.

Single-tilt rotation holders can sometimes be advantageous (e.g., to line up interfaces in certain directions) and again are best if they can be cooled and are low background (for XEDS).

*Second, which kV should you use?* In diffraction, unlike most other TEM techniques, there is often an advantage to using lower kVs since the elastic-scattering cross section is higher. So the patterns are more intense. Also the Ewald sphere is more curved at lower kVs and so it intercepts more electrons scattered at higher angles than those in the ZOLZ. However, higher kVs give higher-resolution information from smaller volumes of your specimen and you can 'see' through thicker specimens. So you may have to compromise and gather patterns over a range of kVs.

Third, how thick should your specimen be? As we already mentioned, unlike most other TEM techniques, thicker specimens can be more useful than thinner specimens since more dynamical scattering occurs. Much of the undesirable diffuse scattering that hides the dynamical information can be filtered out in an EFTEM (much more about this later and in Section 38.2).

### 20.2.A Comparing SAD and CBED

Now let's consider the differences in the electron optics of SAD and CBED. In SAD the electron beam incident on your specimen is parallel (fixed incident vector  $\mathbf{k}$ ) and relatively large (usually  $\sim 1\text{--}10\ \mu\text{m}$  in diameter). In CBED, the beam is convergent (range of  $\mathbf{k}$  vectors) and relatively small (usually  $\sim 1\text{--}100\ \text{nm}$  in diameter) as shown in Figure 20.1. (Compare this situation with Kikuchi patterns which are generated by a divergent beam of electrons within the specimen.) We've already seen in Chapters 11 and 16 that parallel illumination means that the SADP consists of an array of sharp maxima (or spots) in the BFP of the objective lens and, as mentioned in Chapter 9, the beam convergence in CBED gives rise to a pattern of disks of intensity. Figure 20.2A shows an SADP from pure Si and Figure 20.2B is a CBED pattern from a much smaller region of the same Si specimen. While it isn't obvious that the CBED pattern comes from a smaller region of the specimen (i.e., has better *spatial* resolution), you can certainly see that it contains a wealth of contrast detail not present in the SADP. The dark lines within the 000 disk and between the diffraction

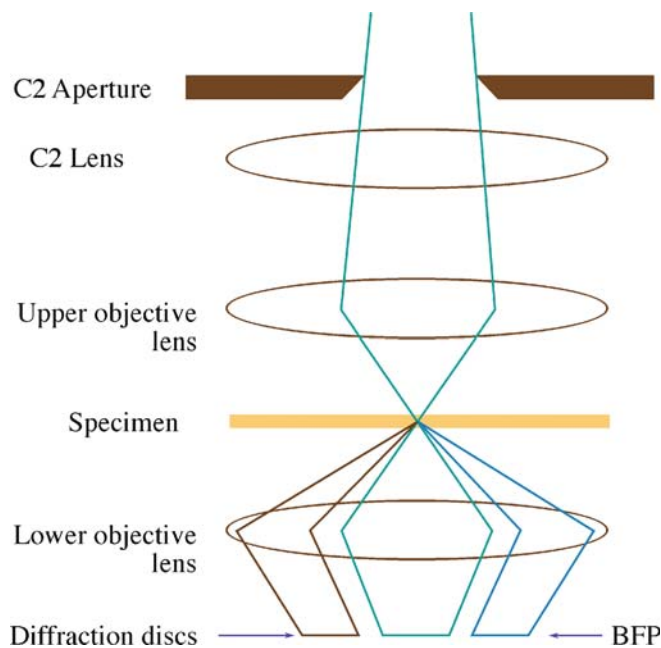


**FIGURE 20.1.** Ray diagram showing CBED pattern formation. If the c/o lens system focuses the beam at the specimen, the illuminated area is very small compared with parallel-beam SADP formation. A convergent beam at the specimen results in the formation of disks in the BFP of the objective lens.

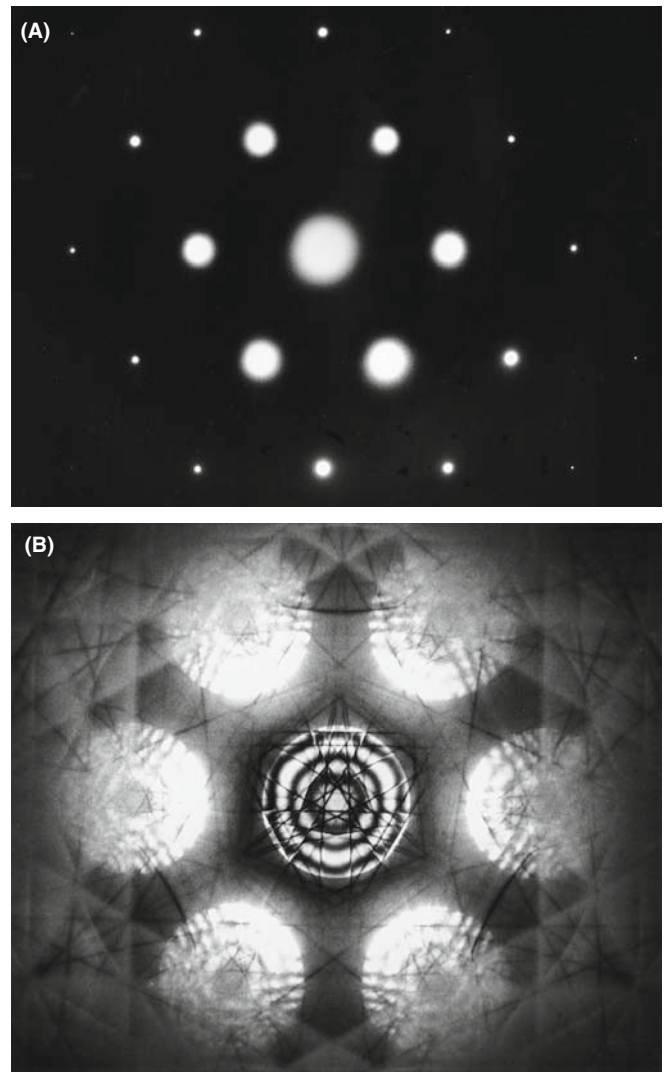


**FIGURE 20.2.** (A) SADP from [111] Si showing the first few orders of diffraction spots and no visible Kikuchi lines. (B) CBED pattern from [111] Si showing dynamical contrast within the disks as well as diffuse Kikuchi bands and sharp, deficient HOLZ lines.

disks are HOLZ effects which we'll return to many times throughout this and the next chapter. Converging the beam, in effect, opens up a greater angular range of reciprocal space for you to look into and in doing so it reduces the *angular* resolution of the DP (which is not something we worry about too much).

#### RELATING SAD AND CBED

You can imagine CBED as magnifying the information within the spots in the SAD. Like SAD, CBED is most useful when you either orient the beam along a zone axis in the crystal to give a symmetrical zone-axis pattern (ZAP) or when you tilt to strong two-beam conditions. Unlike SAD, CBED is also even more useful when the probe is deliberately under- or overfocused.

From Figure 20.1 you can see that we need a condenser/objective (c/o) lens (i.e., a strong upper-objective polepiece) to create a convergent beam, so any probe-forming TEM or dedicated STEM can generate such patterns. We've already described the lens systems and ray diagrams associated with forming a convergent beam in Chapters 6 and 9, so here we will emphasize the experimental variables that you can control. The various steps we describe below are covered in far greater detail, both operationally and in terms of extraordinarily detailed ray diagrams, in the essential text by Morniroli. We'll start with TEM mode and then describe STEM operation.

## 20.2.B CBED in TEM Mode

It's a good idea to start practicing CBED with a thin, single-crystal Si specimen or a stainless steel foil with large grains, since these specimens give immediately useful patterns containing many of the features that we'll be describing (without the need for cooling). The Si is a little easier since the parent wafer will be in a specific orientation such as  $\langle 111 \rangle$  and you'll invariably get a pattern like Figure 20.2B.

When you converge the beam in image mode, you'll lose any useful image contrast and you'll just see a bright spot on the TEM screen or computer display. But if you aligned the condenser system correctly then the beam will be focused on the region you chose. You will develop your own procedure as you gain experience. Basically the approach is as follows:

- Start with your specimen in the eucentric plane, as usual. Weaken C2 to give a broad, parallel beam, then focus an image with the feature from which you want to obtain the CBED pattern in the middle of the screen. It helps if you can do this without the objective diaphragm inserted. If you need it, then you'll have to take it out later (see below).
- Select a large C2 aperture about 100–200  $\mu\text{m}$  in diameter, carefully center it, then adjust the C2 lens to converge the beam to a focused spot on the area of interest.
- Keep C1 weakly excited to give a relatively large spot, about 100 nm FWTM (see Chapter 5) which should contain sufficient current to give a high-intensity pattern.
- Select a small camera length,  $< 500$  mm to give a wide-angle view of the pattern.
- To observe the CBED pattern, just switch to diffraction mode, making sure the objective and SAD diaphragms are retracted.

Remember that you control the minimum illuminated area on the screen (i.e., the beam diameter at the specimen) by the strength of the C1 lens, so after these initial steps, you might want to select a smaller probe size by increasing the C1 strength.

## 20.2.C CBED in STEM Mode

You should first get a focused STEM image of the specimen as we described in Section 9.4.

The procedure is quite simple because in STEM you're always operating with a focused probe and you don't have imaging-system diaphragms to worry about

- First, stop the beam scanning (i.e., select 'spot' mode on the STEM control system).
- Second, position the spot on the STEM screen on the region of interest.

A CBED pattern should then be visible on the TEM screen, but to see it you may have to remove the STEM detector if it sits above the TEM screen, or lower the TEM screen if the detector is below. The CBED pattern is present because the TEM is operated in the diffraction mode during STEM operation. As before, you may have to reduce  $L$  to ensure that several orders of diffraction maxima are visible on the screen. The other variables are the same, except that in STEM, the C2 lens in some TEMs is automatically switched off. This means that the C2 aperture alone governs  $\alpha$  and you can only focus the pattern with the objective lens.

### STEM AND CBED

In TEM you can't see the area of the specimen you have chosen without spreading the convergent beam; in STEM you can always scan the convergent beam to see the image.

In a DSTEM you can see both image and DP at the same time because the CBED pattern can be viewed by introducing a screen after the last post-specimen lens and viewing this screen with a TV camera. A hole in the screen allows any selected portion of the pattern to travel through the EELS to the BF detector and thus both image and DP can be viewed simultaneously. If you don't have post-specimen lenses then you can't vary  $L$ ; the CBED pattern is then viewed either directly using a TV camera to image the BFP of the objective lens or by scanning the pattern across the BF detector using post-specimen scan coils (see Section 21.8).

If you send the CBED pattern through the EELS before viewing it, then you can switch on the EELS and use it to filter out energy-loss electrons, or form the patterns with electrons of a specific energy. Energy-filtered CBED (which you can do in a TEM as well as a STEM) is a most powerful technique, as we'll see (look ahead to Figure 20.10).

The choice of operating mode then is really up to you; TEM and STEM both have their advantages.

## 20.3 EXPERIMENTAL VARIABLES

To form CBED patterns, you have to create a small ( $< 100$  nm) beam with a convergence semi-angle ( $\alpha$ )  $\geq 10$  mrad. There are at least five microscope variables you need to control when forming a CBED pattern

- The beam-convergence angle  $\alpha$  (remember, we mean semi-angle)
- The camera length  $L$  (i.e., the magnification of the pattern)
- The size of the beam (the probe diameter)
- The thickness of the specimen
- The focus of the pattern (under/over or exact)

The last variable is the most complex because there are CBED techniques which require focused patterns and those where we deliberately defocus the beam out of the specimen plane to gain other advantages. So we'll deal with this last variable separately. You can also change the kV if you want and as we noted above, low kV gives better contrast, but this is more than offset by the drop in gun brightness and the increased beam spreading. So, for materials specimens, most CBED is done at the highest kV, as with most other TEM techniques.

### 20.3.A Choosing the C2 Aperture

After you've read the next few sections you'll probably conclude that any full CBED study should include patterns taken with a range of camera lengths, a range of exposures, a range of C2 apertures and that the more C2 apertures you have in your TEM the better. You'll be right on all counts!

Once the CBED pattern is visible on the screen you can adjust  $\alpha$  by changing the C2 aperture, making sure to center the aperture you finally choose. The size of the diffraction disks depends on  $\alpha$  as shown in Figure 20.3 (go back and check equation 5.6). Let's start by choosing a small aperture so we get a pattern of discrete disks, similar to an SADP and we'll use the terminology first introduced by Steeds.

#### KOSSEL AND MÖLLENSTEDT

The pattern of non-overlapping disks is a Kossel-Möllenstedt (K-M) pattern. The pattern of completely overlapping disks is a Kossel pattern.

To get a K-M pattern you must select a C2 aperture such that the disk size (governed by  $\alpha$ ) is less than the spacing of the disks (governed by  $\theta_B$ ) for the particular specimen and orientation. Typically, the Bragg angle is a few milliradians, and C2 apertures in the 10–50  $\mu\text{m}$  range will usually ensure that you have satisfied the K-M conditions.

If  $\alpha$  is large enough for substantial overlap of the disks to occur such that individual diffraction maxima are no longer discernible, then the term 'Kossel pattern' is used (although this can cause confusion with the classic use of the term for geometrically similar X-ray patterns). Figure 20.3A–C shows a series of ray diagrams illustrating the transition from a K-M pattern to a Kossel pattern by increasing  $2\alpha$ . Equivalent experimental patterns from pure Al are shown in Figure 20.3D–F. The patterns in Figure 20.3 were all taken at a small camera length and, although the contrast is not particularly strong, you can clearly see rings of intensity which arise from electrons scattered to quite high angles ( $\pm 10^\circ$ ). We'll continue to read more about these HOLZ diffraction effects throughout this chapter.

Kossel patterns are most useful when viewed with a small camera length (see next section) because they display a relatively extensive area of reciprocal space, and the large value of  $\alpha$  gives rise to Kikuchi bands. For reasons we'll describe in Section 20.7, Kikuchi lines are much more prevalent in CBED than in SADPs and don't require the usual thick specimen. As we described in Chapter 18, the Kikuchi bands intersect in the center of the pattern when the beam is incident down a zone axis, as you can see in Figure 20.3F. Thus it is very easy for you to tilt to a particular zone axis, simply by following the bands until they intersect. So, to form a ZAP, it is best to start at very small  $L$  with a large  $\alpha$ . Later, you can worry about the best choice of C2 aperture, best choice of  $L$  and focusing the pattern. Because these Kossel patterns cover a large angular range in reciprocal space they are also an example of a whole class of large-angle CBED or LACBED patterns (see Section 20.4.B below) in which we defocus the beam to enhance the contrast compared with the Kossel patterns.

Because we need to be able to vary  $\alpha$ , a range of C2 apertures from about 10  $\mu\text{m}$  up to 200  $\mu\text{m}$  is desirable, consistent with the needs of other techniques. A reasonable choice if you have only three C2 apertures: one of about 200  $\mu\text{m}$  for routine TEM, EELS and Kossel patterns, a 50–70  $\mu\text{m}$  ultra-thick aperture for XEDS (which can also be used for STEM imaging and some K-M patterns) and a 10–20  $\mu\text{m}$  aperture for most K-M patterns. Some TEMs provide more than three apertures. More is better!

Because the C2 lens is excited in TEM mode, you can use it to change  $\alpha$ ; if you do, the objective lens has to be changed to maintain a focused pattern. You need to adjust C2 if you change the beam size with the C1 lens or if you want a value of  $\alpha$  between those given by the fixed C2 apertures.

#### STAY IN FOCUS!

Use the specimen-height ( $z$ ) control to maintain the specimen in the eucentric plane as you tilt. A computer-controlled stage is a great advantage.

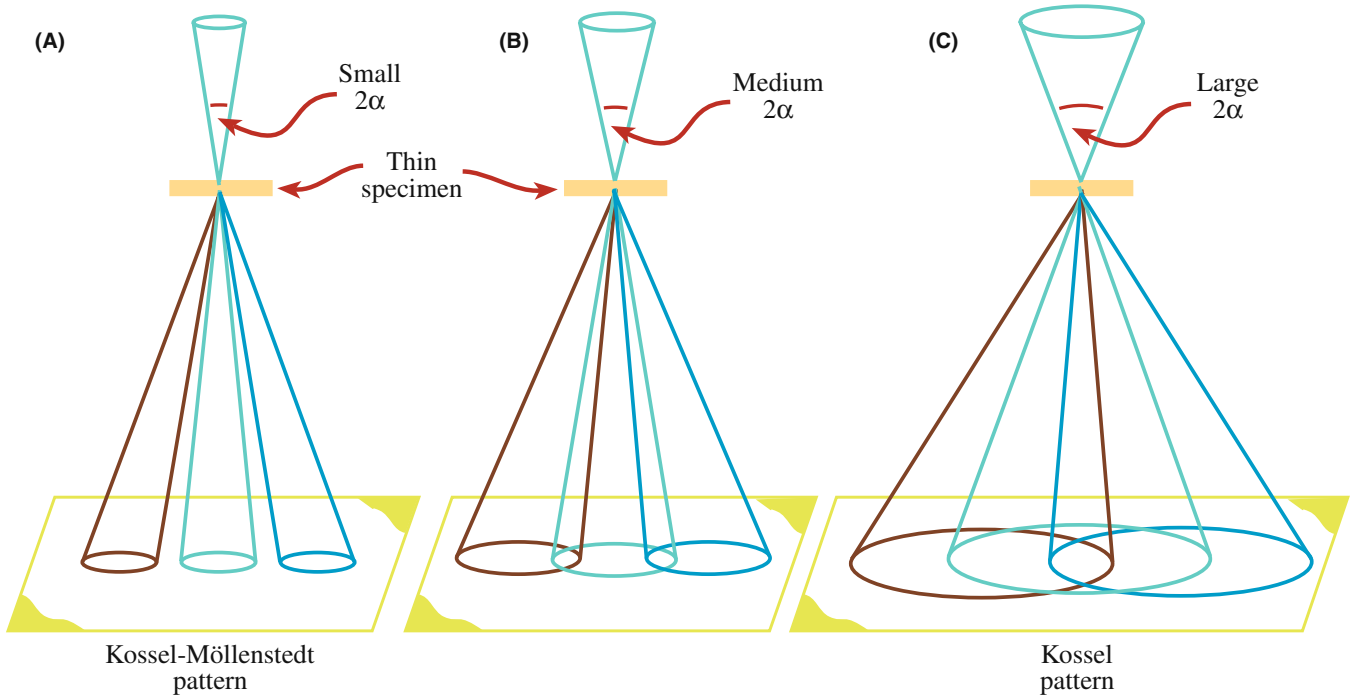


**FIGURE 20.3.** (A–C) Ray diagrams showing how increasing the C2 aperture size causes the CBED pattern to change from one in which individual disks are resolved (K-M pattern) to one in which all the disks overlap (Kossel pattern). (D–F) You can see what happens to experimental CBED patterns on the TEM screen as you select larger C2 apertures.

If you need to know the value of  $\alpha$ , you should use a known crystal to calibrate its variation with C2 aperture size for typical C2 lens excitations, as we described back in Section 9.1 and in equation 5.6.

### 20.3.B Selecting the Camera Length

The choice of  $L$  depends on the information that you want to obtain from the pattern and it's easy to be confused because  $L$  controls the magnification of the DP.

Typically we adjust the post-objective lenses in the imaging system to give  $L > 1500\text{--}6000\text{ mm}$  when we want to observe detail in the 000 (BF) disk at the highest

possible magnification. We reduce  $L$  to  $< 500\text{ mm}$  to view the low-magnification pattern, sometimes called (not surprisingly) the 'whole pattern' (WP) that contains electrons scattered out to high angles. Figure 20.4 shows three CBED patterns obtained over a range of  $L$  and you can see that if we start at a high  $L$  we can only see the 000 disk (Figure 20.4A), then we see the array of ZOLZ disks that is equivalent to an SADP (Figure 20.4B) but at the smallest  $L$  the HOLZ diffraction effects that we just mentioned become visible as a ring of intensity at high angles (Figure 20.4C). So it's often necessary to record your CBED patterns over a range of  $L$  (in addition to a range of  $\alpha$ ).

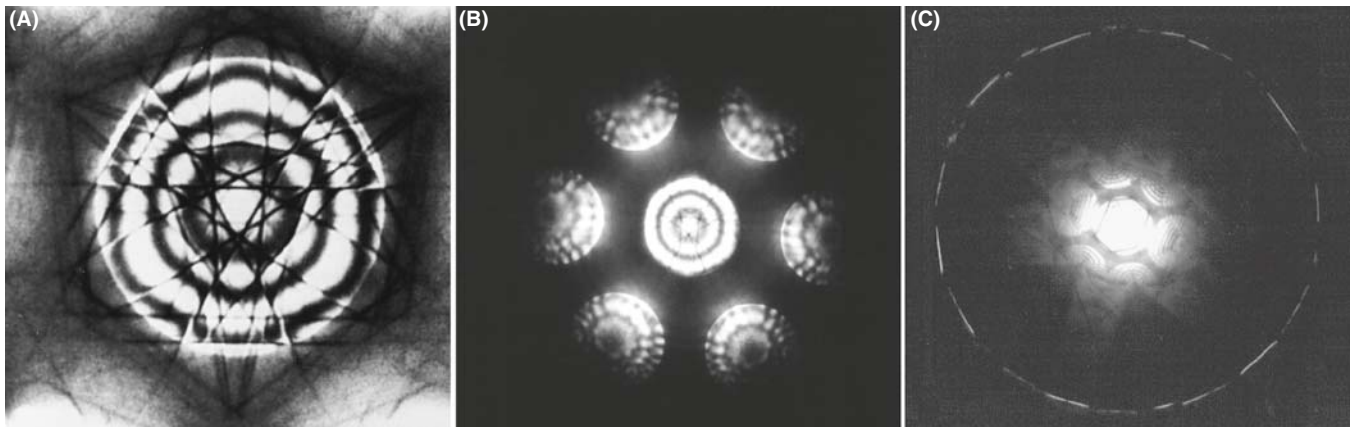


**FIGURE 20.4.** *Decreasing* the camera length,  $L$ , *increases* our view of reciprocal space. (A) Starting at high  $L$ , we see a CBED pattern containing only the 000 diffraction disk. As  $L$  decreases, we see in (B) the distribution of electrons in the ZOLZ, similar to a typical SADP. At the shortest camera length, (C) a ring of HOLZ intensity is faintly visible surrounding the bright ZOLZ disks. Typically, we can record electrons scattered over an angular range of  $\pm 10^\circ$ .

### LARGE $L$ , SMALL ANGLE

A large  $L$  gives a *high*-magnification view of the pattern but only spans a *small* angular range of reciprocal space.

In dedicated STEMs that don't have post-specimen lenses, the CBED pattern is projected onto the BF and/or ADF detector at a fixed magnification.

### 20.3.C Choice of Beam Size

We've already mentioned that you should start with a reasonably large beam with enough current to give a good intense pattern on the screen. Of course, a large beam size doesn't help if the crystal you're trying to analyze is small. The volume sampled by the beam defines the spatial resolution and so it is important to control the beam diameter. For the thinnest specimens, spatial resolution is close to the beam size but, in thicker specimens, elastic scattering will spread the beam and degrade the resolution in a manner similar to XEDS (see Chapter 36). Using the thinnest specimens and an FEG, CBED patterns can be obtained from extraordinarily small regions; we'll see in Section 21.8.B that sub-nanometer diffraction is possible. However, there is a drawback to using the thinnest specimens because they don't exhibit dynamical-diffraction effects which, as you'll soon see, are really useful.

### 20.3.D Effect of Specimen Thickness

If your specimen is very thin you may have kinematical-diffraction conditions. Then the diffraction disks have a uniform intensity and are devoid of contrast, as shown in the ZAP in Figure 20.5A. Moving to a thicker area of the specimen in the same orientation transforms the

pattern from an array of kinematically bland disks to a display of striking dynamical contrast (Figure 20.5B), which we'll discuss in great detail. So to get the most out of a CBED pattern, your specimen should be thicker than one extinction distance (see Chapter 16). As we've now mentioned many times, this requirement differs from that of almost all other TEM techniques, such as HRTEM, XEDS and EELS where the best information is obtained from the thinnest foils. So if your specimens are too thick for anything else, you can almost always get something useful out of them with CBED! As we'll discuss in Section 20.5, you can always energy-filter your CBED patterns from thick specimens and reduce the diffuse-scattering background to enhance the useful dynamical contrast.

## 20.4 FOCUSED AND DEFOCUSED CBED PATTERNS

There are times when you need to focus the CBED pattern and times when you have to defocus it. If you think about it, a focused CBED pattern will always come from the smallest possible region of your specimen and if you don't focus your patterns you will miss a lot of the fine detail! However, if the beam is defocused then what happens is that some image information appears in the CBED pattern (in an equivalent way to creating multiple DF images, which we used to calibrate the SADP rotation back in Section 9.6). Thus, in defocused CBED techniques we sample both direct and reciprocal space. In addition, slightly defocusing the objective lens increases the contrast in the patterns. Both of these advantages turn out to be particularly useful for direct analysis of crystal defects such as dislocations and grain boundaries using large-angle CBED (LACBED).

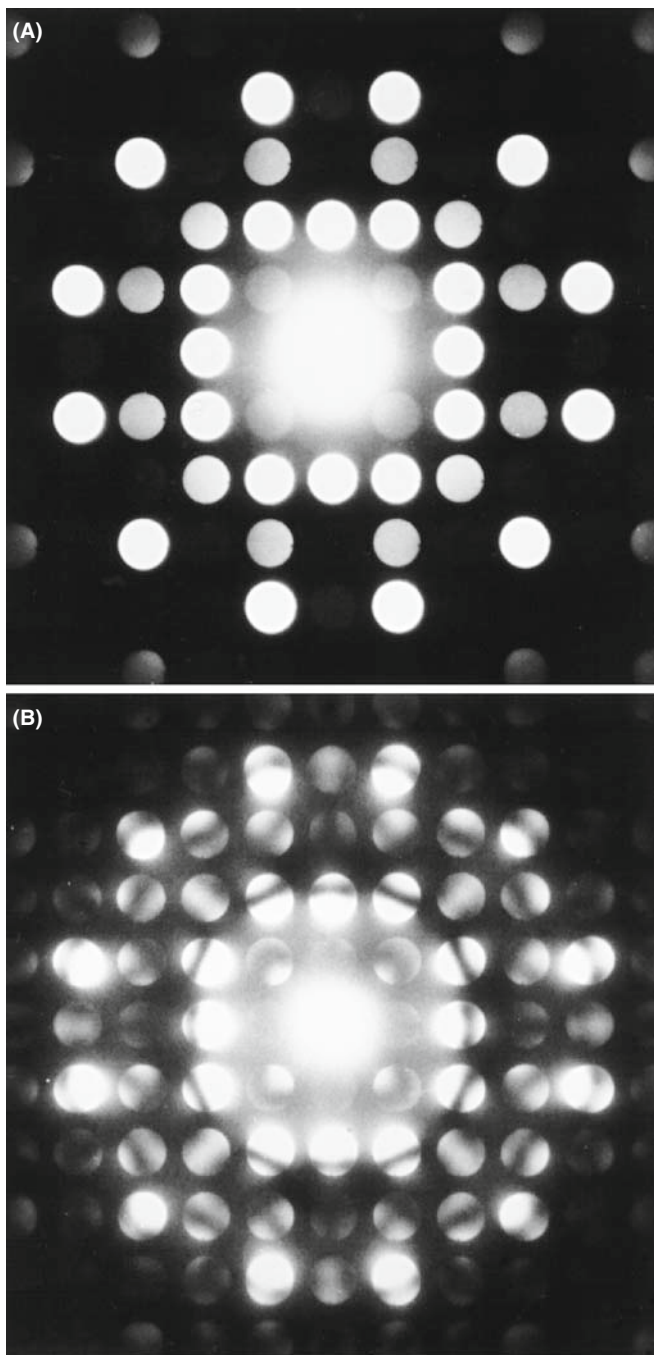


**FIGURE 20.5.** (A) CBED pattern under kinematical conditions. Such patterns give us no more information than SADPs, and their only advantage over SAD is that they come from a smaller region of the sample. (B) CBED pattern from a thicker area of the same specimen in (A) showing detailed dynamical-contrast phenomena.

### 20.4.A Focusing a CBED Pattern

Your TEM image is focused if your specimen is at the eucentric height and you can adjust the C2 lens to form the smallest spot on the TEM screen before switching to diffraction mode. To focus the CBED pattern

- Select K-M conditions (choice of C2 aperture) and choose a value of  $L$  so you can clearly see the 000 disk.
- Deliberately underfocus (weaken) the objective lens until a BF image is visible in the disk. This is because the beam is now spread at the plane of the specimen; see Figure 20.6A and the equivalent ray diagram back in Figure 6.5C.
- Strengthen the objective lens. As the beam crossover moves toward the specimen plane the image expands to higher magnifications until it goes through an inversion point at exact focus (see Figure 20.6B, which is equivalent to Figure 6.5B).
- Overfocus and again you can see a BF image in the 000 disk, inverted with respect to the underfocused image (Figure 20.6C). As you can see in Figure 20.6B there is non-spatial (i.e., diffraction-contrast) information in the 000 disk when you are at focus. (As we'll see in the next section, there are in fact several CBED techniques which deliberately use either an under- or overfocused beam).

If you leave the objective-lens current fixed and focus the beam on the specimen by adjusting C2 you'll see a similar effect to that shown in Figure 20.6, because the two lenses are coupled in a c/o system. If you use the second (non-eucentric) tilt axis or move to another region of the specimen, you will probably have to refocus the pattern with the  $z$  control, unless you have a stage that is fully computer controlled.

#### OBJECTIVE LENS CURRENT

Know the value of the objective-lens current that focuses the beam at the eucentric plane in your TEM. If your CBED pattern is focused at a different value, then adjust the lens current and refocus with the  $z$  control to maintain eucentricity.

The CBED pattern also has to be correctly focused in the BFP and you can do this in the conventional manner using the intermediate-lens fine focus to sharpen the image of the C2 aperture. As you'll see, you can also defocus the pattern by moving the specimen above or below the eucentric plane and this is just fine, unless you need to tilt the specimen to set up specific diffraction conditions, in which case the loss of eucentricity can make tilting tedious because the image will shift as you tilt.

### 20.4.B Large-Angle (Defocused) CBED Patterns

The reason we want to defocus the objective lens is that in some cases, as with TEM images, the contrast is minimized

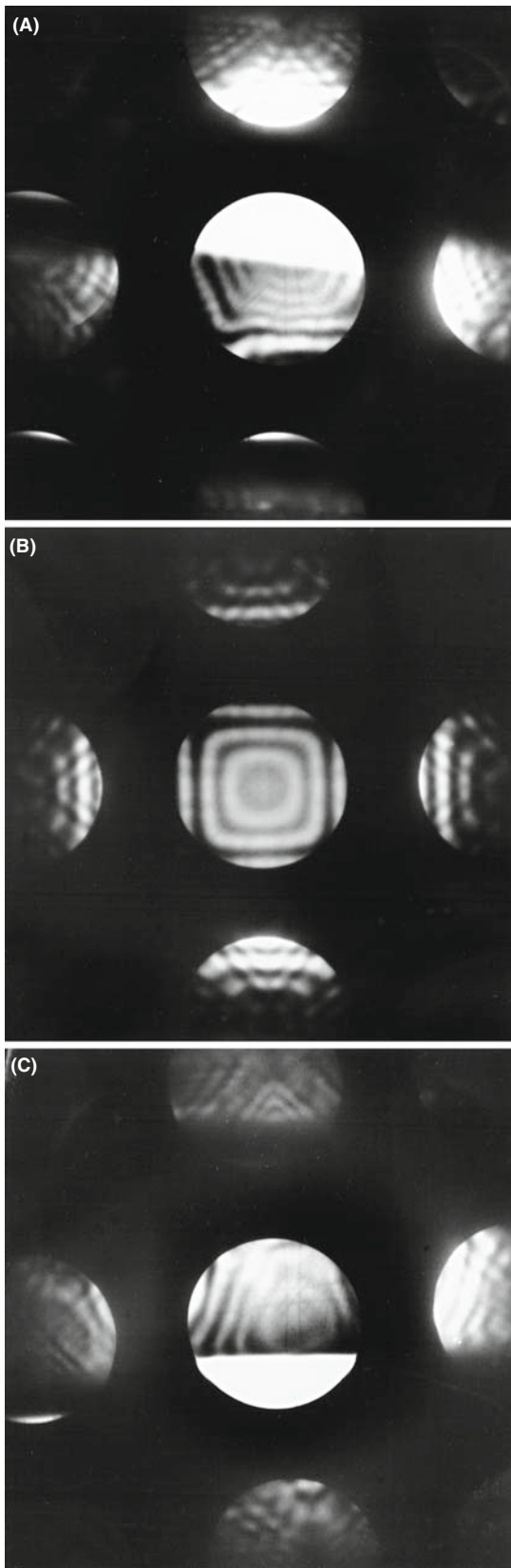


**FIGURE 20.6.** The procedure for correctly focusing the CBED pattern by adjusting the strength of the c/o lens through focus. In both underfocus (A) or overfocus (C) conditions, you see a BF image in 000 and DF images in the  $hkl$  disks, but at exact focus (B) the disks contain non-spatial, dynamical, diffraction contrast. Compare with Figure 6.5.

at exact focus. This is clear if you go back and look at the focused Kossel pattern in Figure 20.3F. At exact focus, the defect and excess Kikuchi lines overlap and reduce the overall contrast as shown in Figure 20.7A (although at the edge of the pattern, (i.e., where the electrons are traveling far off axis.) spherical aberration improves the contrast; a rare advantage for this otherwise-limiting lens defect). However, if you defocus the objective lens (either over or under) then the contrast in that same Kossel pattern is increased remarkably, as shown in Figure 20.7B. This

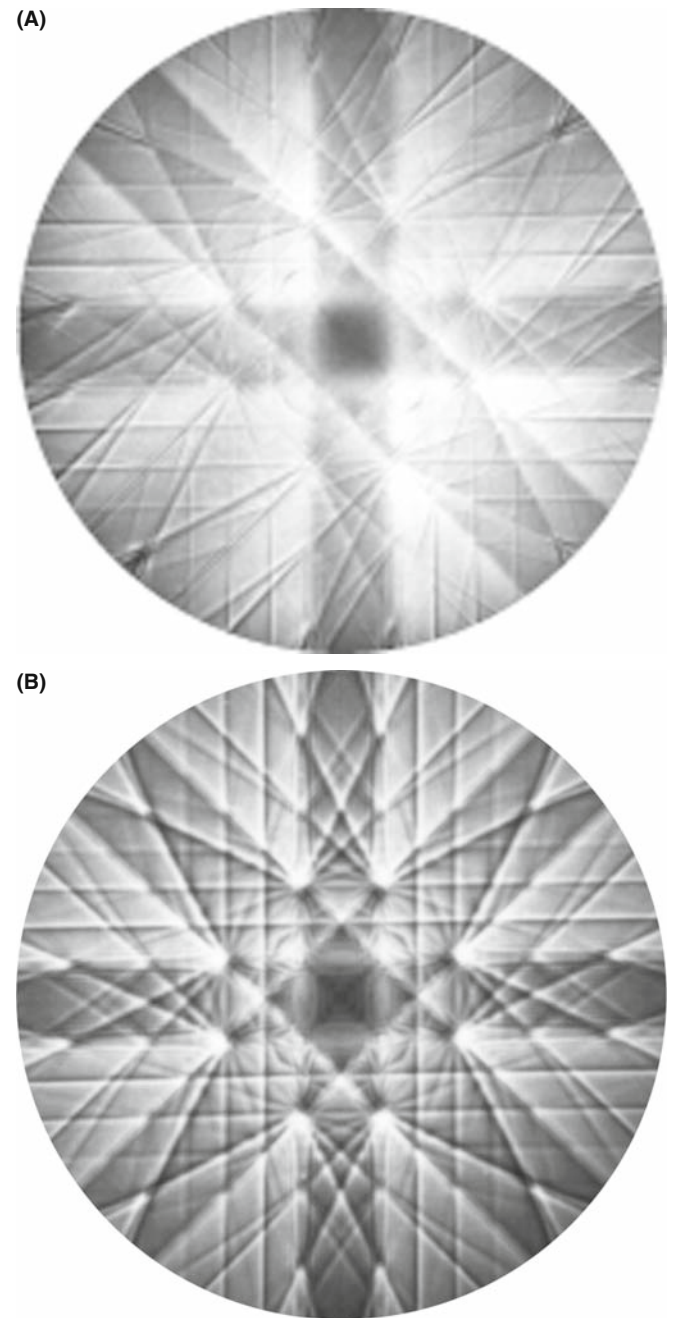


**FIGURE 20.7.** Kossel pattern from Si with the beam down a  $\langle 001 \rangle$  zone axis at (A) exact focus and (B) with the diffraction lens weakened to view a plane before the BFP of the objective lens (i.e., overfocus).

novel approach was pioneered by Tanaka and co-workers in Japan (see the references). There are several forms of defocused CBED patterns and we'll summarize three here and show you some applications of the techniques in the companion text.

The first and most common defocus technique is large-angle CBED or LACBED (Tanaka et al. 1980). These patterns are extraordinarily useful, as a perusal of Morniroli's book will confirm, and they are invaluable in analyzing line and planar crystal defects such as dislocations and interfaces (e.g., Spence and Zuo). There are a couple of ways that you can form LACBED patterns but they are based on Kossel patterns which, as we've noted, display the largest area of reciprocal space because they use the largest possible C2 aperture. Now if you want to defocus the pattern, as we just described in Figure 20.6, it's simple enough: you can either change the height of your specimen by adjusting the  $z$  control on the stage or you can defocus the C2 lens so that the beam does not form a crossover in the plane of the specimen as shown schematically in Figure 20.8A. This is a beautiful but initially daunting diagram, characteristic of many by Morniroli, but well worth taking the time to understand.

Start by looking at the cone of incident electrons in which two planes (ABE and CDE) are indicated where the electrons satisfy the Bragg condition for  $\pm hkl$  and these planes are bisected by the trace of the  $hkl$  plane itself. The beam is focused on the object plane of the objective lens and the specimen is raised a distance  $\Delta h$  out of that plane so it is illuminated by a disk of intensity. This has the effect of separating out the  $\pm \mathbf{g}_{hkl}$  diffracted electrons. The electrons incident along the lines  $A_E-B_E$  and  $C_E-D_E$  are Bragg diffracted and form  $\pm \mathbf{g}_{hkl}$  diffraction spots at K and L, respectively, in the object plane, and the direct-beam electrons form the 000 spot at E. All the electrons diverge through the spots and are re-focused by the objective lens to form spots in the image plane ( $K'$ ,  $L'$ , and  $E'$ ), respectively, and Figure 20.8B shows such a spot pattern. In the BFP there is a LACBED pattern consisting of a disk of intensity crossed by deficient lines (like Kikuchi lines but arising from elastic scattering) which are called Bragg lines (see Section 20.7 below). These deficient lines ( $A_F-B_F$  and  $C_F-D_F$ ) correspond to the lines in the specimen along which strong diffraction occurred from the  $\pm hkl$  diffracting planes as shown in Figure 20.8C and arise from the superpositioning of the  $h\bar{k}l$  excess lines on the  $hkl$  deficiency line ( $A_F-B_F$ ) and vice versa ( $C_F-D_F$ ). As you can see, there are lines from many diffracting planes in this figure while, for simplicity, Figure 20.8A only includes the ray paths for two strongly diffracting planes exactly at  $\mathbf{s} = 0$ .

Figure 20.8A shows that the key to getting the best LACBED patterns is careful use of the SAD

aperture. If you insert an SAD diaphragm into the image plane and permit only the direct beam to go through the aperture, the (BF) LACBED pattern you see on the screen is remarkably enhanced, as shown in Figure 20.8D (compare this with Figure 20.8C which is a LACBED pattern without the SAD aperture inserted). A DF LACBED pattern can be acquired simply by selecting one of the  $\mathbf{g}_{hkl}$  reflections in the image plane with the SAD aperture and such a pattern consists of just a single  $\pm hkl$  excess line of intensity. It is possible to improve the contrast in the LACBED pattern by choosing a smaller SAD aperture to cut out some of the inelastic, higher-angle scattering. If you look carefully at Figure 20.8D, you see that, as in all LACBED patterns, there is some real-space information about the specimen but the reciprocal-space information clearly dominates. Figure 20.9 shows a montage of BF and multiple DF LACBED patterns from Si in the [111] orientation. The beauty of such a pattern is only enhanced by the fact that the symmetry information can be used to determine the point group of the crystal directly; more about that in the companion text.

The second technique is called convergent-beam imaging or CBIM, which is a little younger than LACBED (Humphreys et al.). CBIM saw relatively little use because all it really did was give you an image of the area of your specimen from which you were obtaining the CBED pattern. If you include an objective aperture, a very small spot size and an energy filter the quality of the CBIM patterns is close to that of LACBED patterns although invariably CBIM emphasizes real-space over reciprocal-space information.

The last defocus technique in this acronym soup is parallel recording of dark-field images (PARODI) as a function of specimen thickness. The intensity variation in the multiple DF images visible in a systematic row of diffraction disks of a defocused CBED pattern (Wu et al.) can be recorded in a single exposure and, if you understand a lot of physics, you can use this approach to determine various properties of your crystalline specimens such as structure factors and valence-electron distributions.

There are several other mechanisms for obtaining LACBED patterns summarized by Morniroli, such as eucentric LACBED, specimen rocking, BF and DF LACBED and montages of CBED patterns, the last of which is illustrated in Figure 20.9.

### 20.4.C Final Adjustment

Sometimes, in either defocused or focused CBED patterns, it is quite difficult to make the ZAP exactly symmetrical as in Figure 20.2B. It often seems as if your last

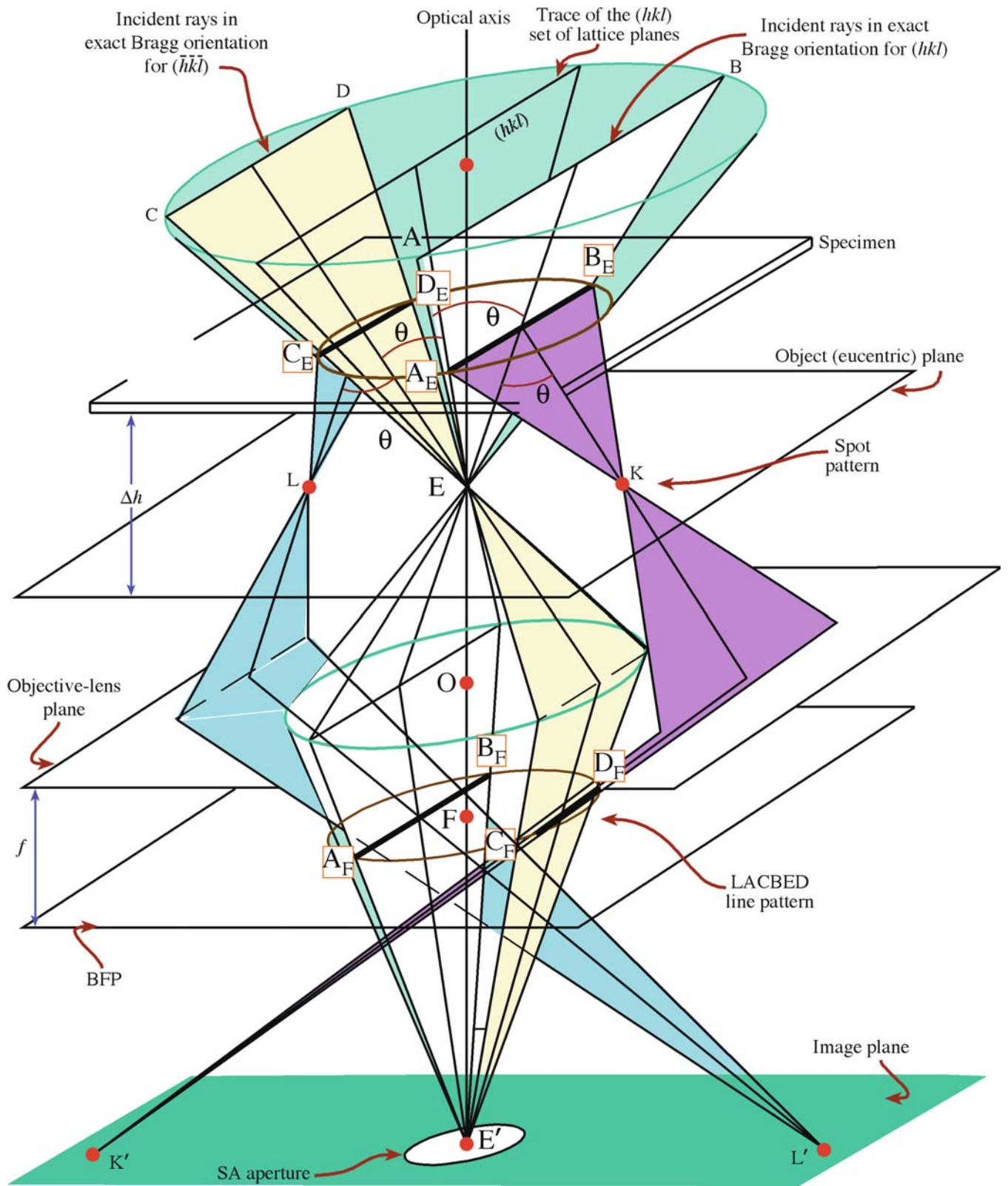
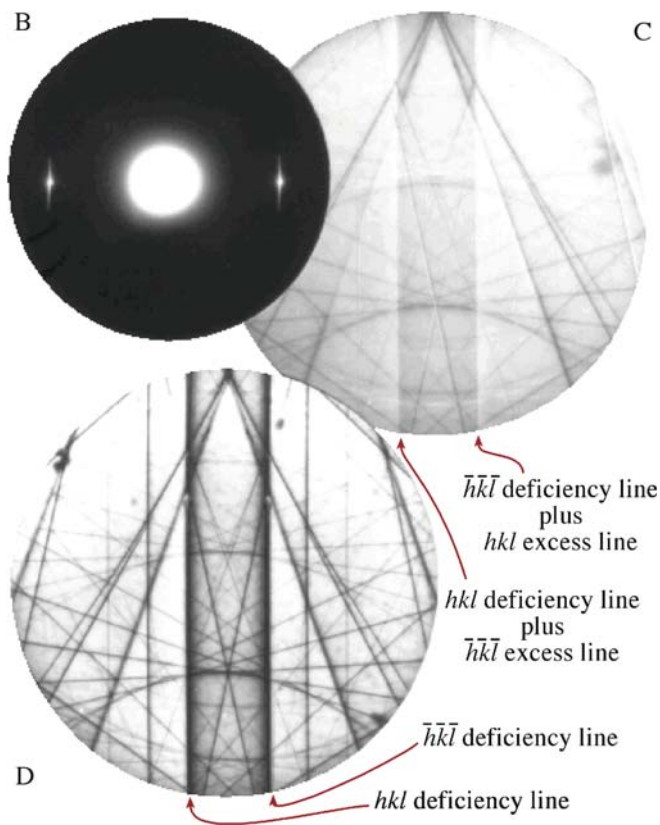


**FIGURE 20.8** (A) Ray diagram for LACBED formation under  $\pm h$  (three-beam) conditions. With the specimen raised by  $\Delta h$  from the eucentric plane in the objective lens, specific electrons in the incident cone are at the exact Bragg condition for diffraction from both sides of the  $hkl$  plane indicated, creating a spot pattern in the eucentric plane (B) and a LACBED pattern of lines in the BFP (C). The SAD diaphragm can be inserted to enhance contrast in the LACBED pattern by selecting only one beam to create (D) a BF LACBED pattern.



- Increase  $L$  to examine the 000 disk and focus the pattern.
- Defocus the pattern with the objective lens or raise/lower the specimen from the eucentric plane if you want to do LACBED, PARODI, CBIM or some form of defocused CBED.

## 20.5 ENERGY FILTERING

Every kind of DP contains electrons that have lost energy in going through the specimen. As we've seen already, these inelastically scattered electrons can be very useful if they cause Kikuchi lines, but if your specimen is thick enough, then the diffuse, inelastic scattering can raise the background intensity to levels that mask the useful contrast in the pattern. This is particularly the case in CBED patterns because, as we noted back in Section 20.2 and Figure 20.5, CBED is one of the few TEM techniques wherein more useful information is present in patterns from thicker specimens because they give rise to much more interesting dynamical contrast within the CBED disks.

So there's a balance here: we want thicker specimens to enhance dynamical effects but if the specimen is too thick the diffuse, inelastic scattering hides the useful contrast. If this is the case we can, in fact, have our cake and eat it at the same time. All we have to do is remove the diffuse-scattered electrons from the pattern using an energy filter.

### TO FILTER OR NOT?

If you can energy-filter your CBED patterns, you should always do so.

Now we'll talk a lot more about energy filtering when we discuss EELS in the last four chapters of Part 4 and the seminal text on filtering is edited by Reimer. Filtering can be achieved either with an in-column or post-column filter. If we remove inelastically scattered electrons, the CBED pattern contains electrons that have lost no energy. Thus, in effect we have removed any specimen-induced chromatic-aberration effects from the pattern, and all the contrast phenomena in the pattern appear much sharper because all the electrons are focused in the (same) BFP (or image plane if it is a LACBED pattern). All this text pales in comparison with the example shown in Figure 20.10. This improvement is so dramatic that it really never makes sense to do anything other than filter your CBED patterns if you have the necessary instrumentation.

FIGURE 20.8. (Continued).

minor tilt or traverse of the specimen is not precise enough, or mechanical backlash occurs. If this is the case, use the beam tilts or deflectors to make your final adjustments to obtain a symmetrical pattern. In Section 18.2, we used the same method to excite high-order reflections in SAD. You can also move the C2 aperture and center it on the zone axis, but this misaligns the illumination system so it should be the last resort.

As with SAD, a range of exposure times for all CBED patterns will give you the most information.

We can now summarize the experimental steps to obtain a CBED pattern

- Focus the beam to a crossover on your specimen at the eucentric plane and go to diffraction mode in TEM (or stop the beam from scanning in STEM).
- Decrease  $L$  to see the full pattern including HOLZ scattering and tilt to the desired orientation.
- Adjust the convergence angle with the C2 aperture.
- Increase the beam size if necessary with the C1 lens to make the pattern brighter.
- Decrease the beam size and/or go to a thinner portion of the specimen to select a smaller region (which generally increases the quality of the pattern).

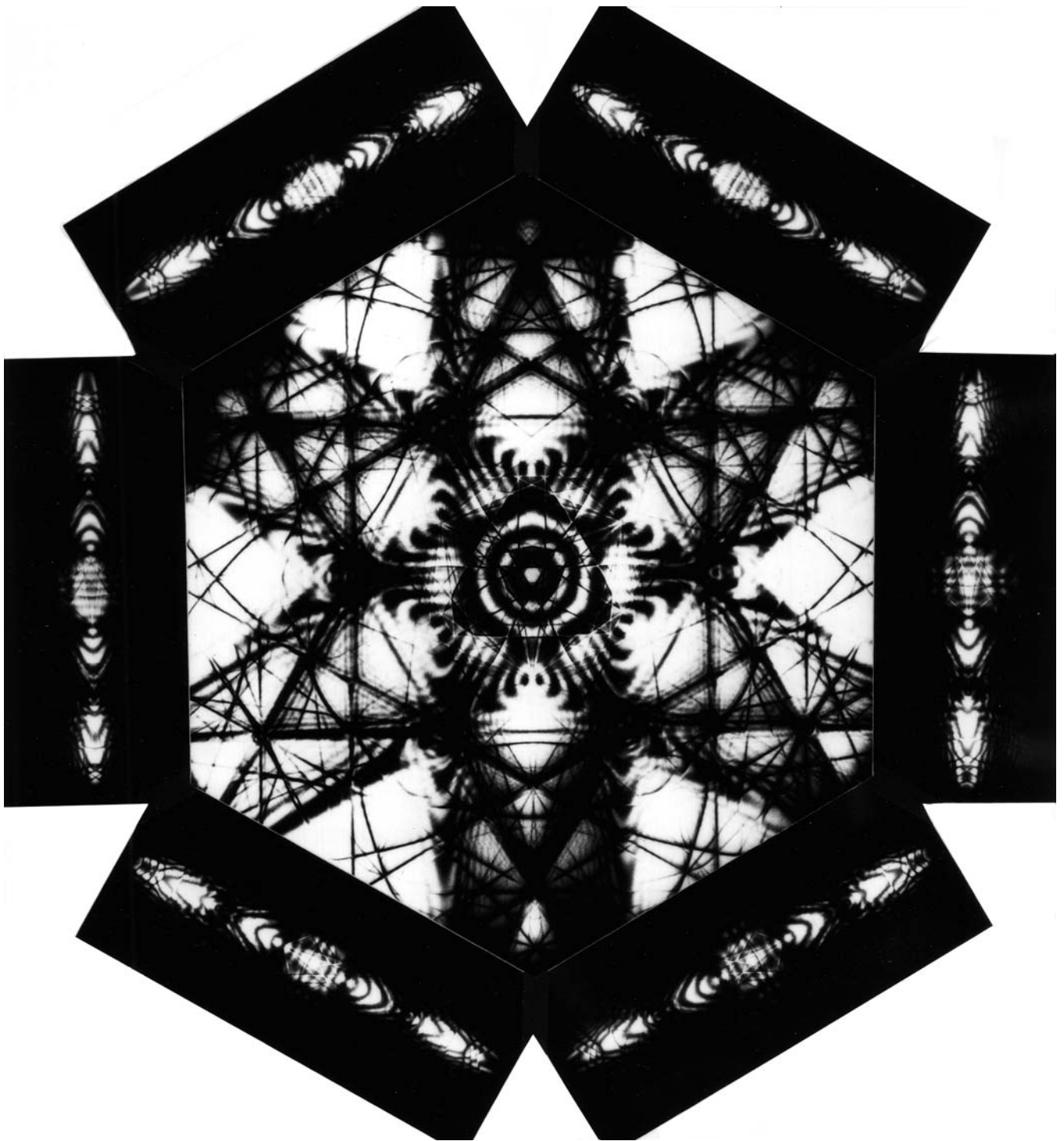


FIGURE 20.9. Montage of Si [111] BF LACBED pattern (center) surrounded by six  $\{2\bar{2}0\}$  DF LACBED patterns.

## 20.6 ZERO-ORDER AND HIGH-ORDER LAUE-ZONE DIFFRACTION

### 20.6.A ZOLZ Patterns

If you increase  $L$  above  $\sim 800$  mm you will magnify the pattern on the screen and only see the first few diffraction maxima, as shown in Figure 20.4A. Assuming the

C2 aperture is small enough, the CBED pattern consists of disks, similar to the array of spots in an SADP, i.e., discrete diffraction maxima surrounding the central 000 disk. Remember that such a pattern is termed a ZOLZ pattern (see Section 18.4) since the permitted  $hkl$  diffraction maxima must all satisfy the Weiss zone law  $hU + kV + lW = 0$ , where  $UVW$  is the beam direction. Remember also that all the  $hkl$  maxima in the DP

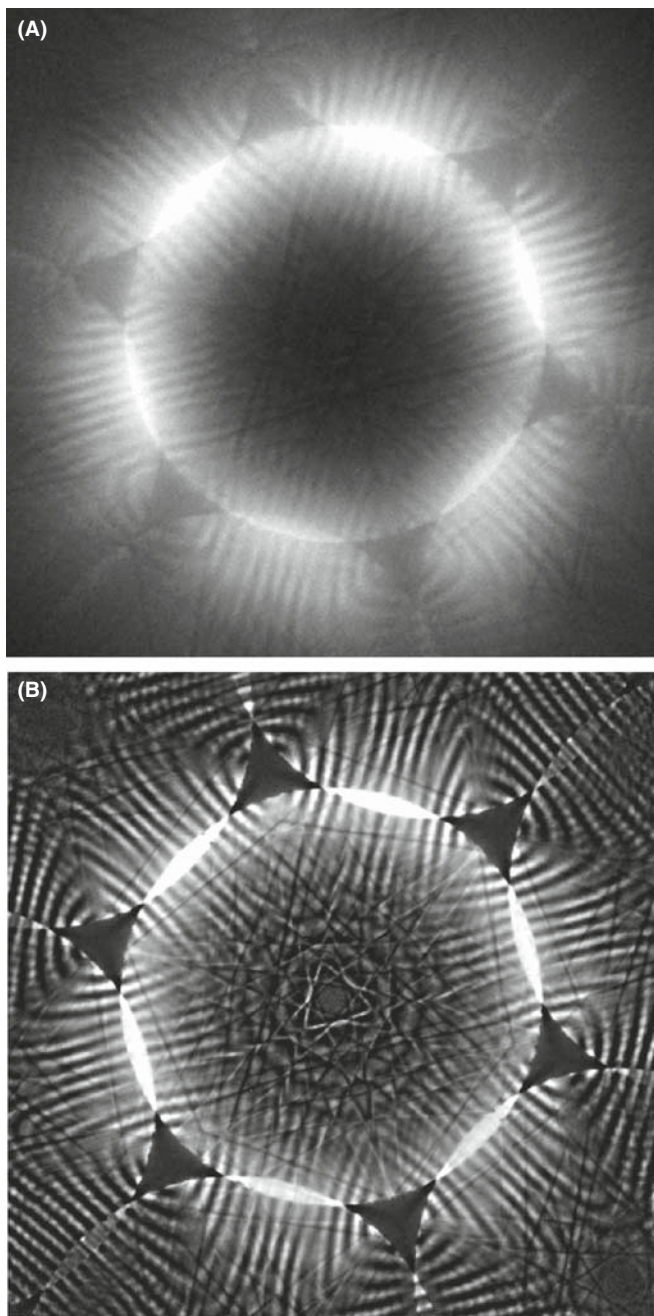


**FIGURE 20.10.** CBED pattern from a thick specimen of Si (A) without energy filtering and (B) with energy filtering. This figure is included only because it looks so striking, and similar patterns have been the basis of many TEM lab Christmas cards.

correspond to points in the reciprocal-lattice plane containing the origin, 000, of the reciprocal lattice, and this plane is also called the ZOLZ. So in fact SADPs are usually ZOLZ patterns, although we don't always describe them as such. From ZOLZ patterns, we can obtain the usual interplanar spacings and angles, the  $hkl$  maxima can be indexed and  $UVW$  identified, in exactly the same manner as we described in Section 18.4 for an

SADP. The two options are the method of ratios or using a calibration standard to determine the camera length.

Because of the finite size of the diffraction disks, you must take care to select equivalent points in each disk when measuring the  $hkl$  spot spacings. If  $\alpha$  is too large (Kossel conditions) you might not see individual maxima and you should then select a smaller C2 aperture (K-M conditions).

### 20.6.B HOLZ Patterns

The central portion of the CBED pattern is bright due to the relatively intense low-angle scattering (go back and check Figure 3.5). At higher angles, the ZOLZ intensity drops because the atomic-scattering amplitude,  $f(\theta)$ , decreases and the Ewald sphere no longer intercepts the relrods from the ZOLZ. However, the intensity increases again when the Ewald sphere intercepts the relrods from the HOLZ reciprocal-lattice points and a circle or ring of diffracted intensity is observed around the ZOLZ pattern as in Figures 20.3D–F and 20.4C. (You should recall that a circle can be defined geometrically as the interception of a sphere and a plane).

If you've chosen a small enough aperture for K-M conditions you'll see a ring of discrete HOLZ spots as in Figure 20.3D while a large C2 aperture gives a HOLZ ring of intersecting lines as in Figure 20.3F. The HOLZ intensity arises from relatively weak high-angle diffraction from crystal planes that are *not* parallel to the beam. Low temperatures increase the HOLZ scattering and also minimize the thermal-diffuse (phonon) scattering that, in some materials with a large Debye-Waller factor, masks the weak HOLZ intensity. So this is why you'll find a liquid-N<sub>2</sub> cooling holder very useful at times. You can't reduce the diffuse scattering via an energy filter because phonon scattering has a very small energy loss ( $\ll 1$  eV) and most of these electrons still contribute to the filtered pattern.

#### SMALL $L$ , LARGE ANGLE

Remember that the radial distance from 000 in a DP is related to the angle of scattering; use a smaller  $L$  to see higher-angle scattering.

Consider the intersection of the Ewald sphere with the reciprocal lattice. The plane of HOLZ reciprocal-lattice points/relrods intercepts the sphere (unlike the zero layer which is tangential to the Ewald sphere). The first ring is called the FOLZ because the possible  $hkl$  reflections satisfy the relationship  $hU + kV + lW = 1$ , and so on. Where the Ewald sphere intersects the HOLZ relrods, diffracted intensity is expected, taking into account the usual structure-factor effects (see the next section).

Because the beam converges on the specimen over an angular range  $2\alpha$ , the Ewald sphere is effectively rotated  $2\alpha$  about the origin, and thus a range of angles along each HOLZ relrod is sampled, as shown in Figure 20.11A. This range of angles manifests itself as the CBED disk reflecting the effective angular broadening of the relrod, as shown in Figure 20.11B. Different interception points on the relrod correspond to different points in the disk as shown in Figure 20.11C. Figure 20.11D shows a K-M CBED pattern containing the expected distribution of diffraction maxima from the Ewald-sphere construction in Figure 20.11A.

### 3D

The most important point to remember is that there is 3D crystallographic information in the CBED pattern whenever significant HOLZ diffraction intensity is present.

We'll make use of this 3D information in the next chapter and in the companion text.

To observe HOLZ rings in addition to the ZOLZ pattern, choose a very small  $L$  ( $< 500$  nm) so that you can see the full angular range of the BFP permitted by the imaging system ( $\sim \pm 10^\circ$ ). As shown schematically in

Figure 20.11A, the Ewald sphere only intercepts relrods in HOLZs many orders of diffraction maxima away from the direct beam. Because of the large scattering angle, the intensity in the HOLZ spots is relatively low and the exposure time to reveal HOLZ maxima is usually long enough to ensure that the ZOLZ is overexposed on the negative (go back and see Figure 20.3). You might be lucky with your thin area; sometimes you can produce reasonable ZOLZ and HOLZ intensity on the same exposure as in Figure 20.11D. But generally, if you're still stuck with recording your patterns on film you will probably have to record at least two DPs: a relatively short exposure for the ZOLZ pattern containing only 2D crystallographic information and a longer exposure for the weak HOLZ reflections containing the 3D information. As we've already said, a range of exposures is useful for *all* DPs.

There are some alternatives

- A CCD camera will give a greater dynamical range making it easier to record a good pattern showing detail at both low and high scattering angles.
- You can use image-processing techniques on your computer to combine differently exposed patterns (see Chapter 31).

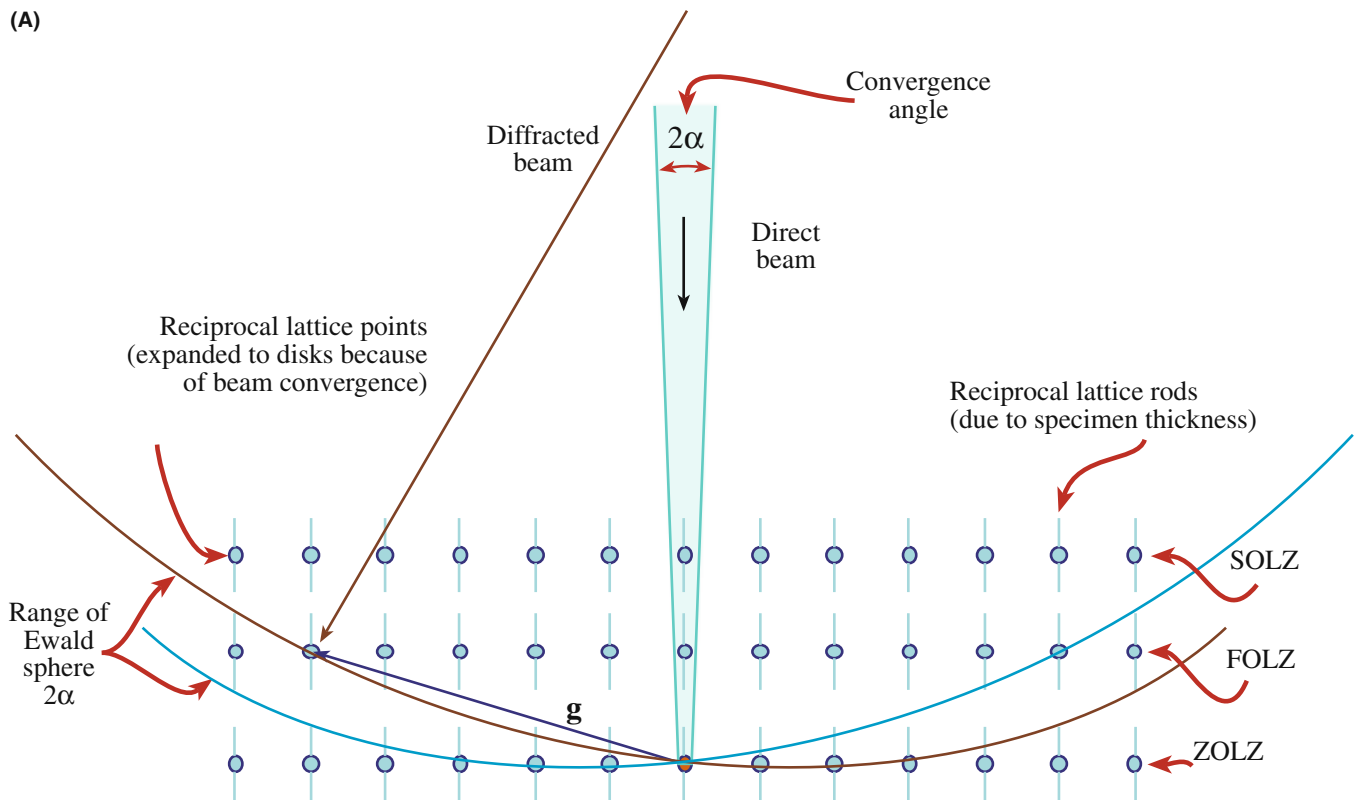


**FIGURE 20.11** (A) The Ewald sphere can intercept reciprocal-lattice points from planes not parallel to the electron beam whose  $\mathbf{g}$  vectors are not normal to the beam. The sphere has an effective thickness of  $2\alpha$  because of beam convergence and so intercepts a range of these HOLZ reciprocal-lattice points.

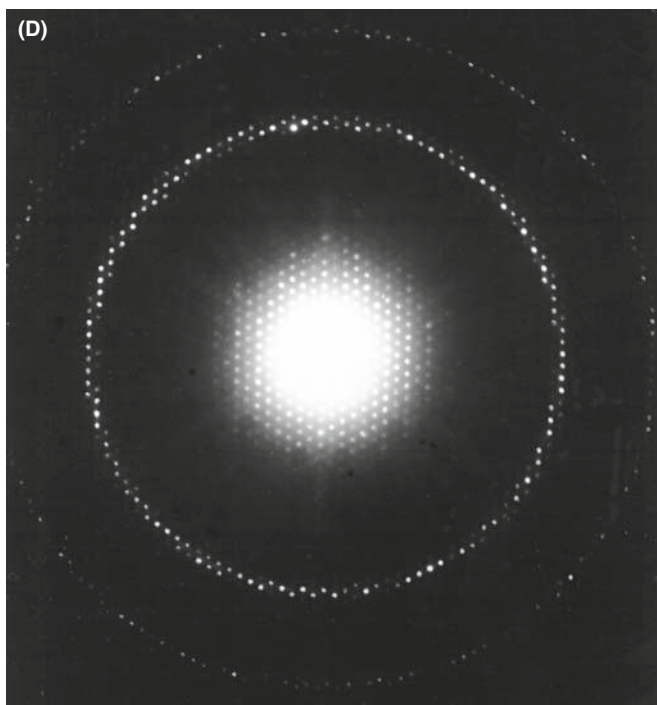
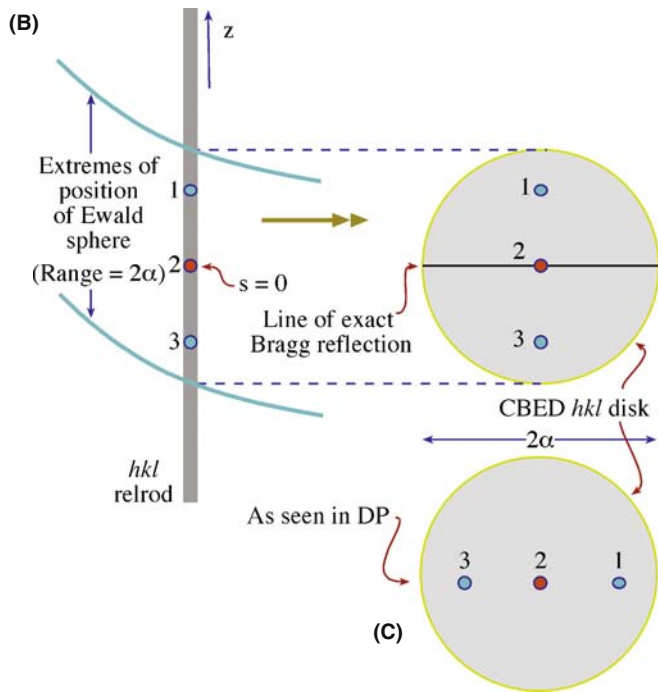


**FIGURE 20.11.** (Continued) The relrod has a shape shown in (B) and the intensity at specific points  $x_i$  in the relrod is directly related to equivalent points in the  $hkl$  disk (C). The interception of the Ewald sphere with the HOLZ layers gives rings: the first ring is called the FOLZ, the second the SOLZ and so on shown in the experimental pattern in (D).

The HOLZ ring radius is defined by the interception of the Ewald sphere with the allowed HOLZ relrods in the reciprocal lattice and so depends on the interplanar spacing in the crystal, the electron wavelength (i.e., the  $kV$ ),  $L$  and any off-axis lens distortion. Depending on

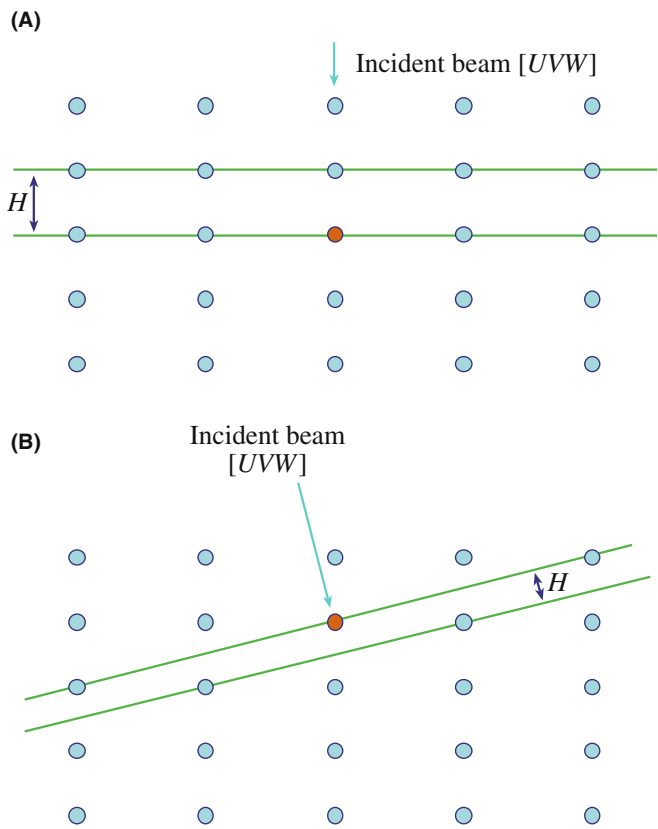


**FIGURE 20.12.** (A) The reciprocal-lattice spacing ( $H$ ) is large if the beam is down a major zone axis in the crystal. (B) The spacing is small if the beam is down a low-symmetry direction.

the crystallography of the specimen, the HOLZ rings may have very large diameters making them difficult to observe experimentally even at very small  $L$ . Under these circumstances, you should tilt to a *low-symmetry* zone axis (e.g.,  $\langle 114 \rangle$ ) since this gives you a better chance of observing the FOLZ than a high-symmetry zone axis such as  $\langle 001 \rangle$ . (If the reason for this is not clear, then look at Figure 20.12.) Cooling your specimen will reduce thermal-diffuse scattering that can mask HOLZ effects. If you still can't see a HOLZ ring, then the last thing you can try is increasing  $\lambda$  by lowering the  $kV$ . If all this fails, you need to pick another specimen!

In the next chapter, we will show you how to index HOLZ patterns and how HOLZ ring measurements can be used to deduce the lattice-repeat vector of the crystal parallel to the beam direction. You'll see that you can then determine the unit cell, the crystal system and also the type of lattice centering.

### 20.7 KIKUCHI AND BRAGG LINES IN CBED PATTERNS

In CBED patterns you almost invariably see sharp Kikuchi lines, while in SADPs Kikuchi lines are often rather diffuse or absent (see Chapter 19). This difference arises

in part because the convergent beam samples a much smaller region of the specimen than that selected by the SAD aperture. So, in the volume of specimen contributing to the CBED pattern, there is usually little or no strain, either elastic (due to specimen bending) or plastic (due to lattice defects). As a result, CBED Kikuchi lines will in general be sharper than SAD lines. This effect is shown in Figure 20.13A which is a conventional SADP containing very diffuse Kikuchi lines. This pattern was obtained from a large region of heavily deformed copper. By comparison, Figure 20.13B shows a CBED pattern from a much smaller region of the same specimen showing several pairs of well-defined Kikuchi lines. So you can use Kikuchi lines in CBED patterns to attack problems which are beyond the capability of SAD, for example, to determine accurate misorientation relationships between small grains in deformed materials (see Heilman et al.). However, if you put the probe right on a defect which has significant strain associated with it then even the CBED pattern may be blurred. On the positive side, this effect is used in LACBED patterns to characterize the crystallography of defects (e.g., the Burgers vectors) and this is explained in detail in the companion text. So, unless you want to study defects, always check the TEM image and tilt around to make sure that the area is clear of defects before getting your CBED patterns.

If the CBED pattern is not a ZAP, as in Figure 20.13B, the Kikuchi lines appear as pairs of excess (bright) and deficient (dark) lines, as in SADPs. But when you obtain a ZAP, the ZOLZ Kikuchi lines appear as bright bands. These bands increase in intensity and definition as you increase the convergence angle, as shown back in Figure 20.3D–F. A similar effect is seen in channeling patterns in the SEM that are generated by rocking a parallel beam around the optic axis. If you need to understand the difference between Kikuchi lines in SADPs and Kikuchi bands in CBED patterns, Reimer gives a clear discourse in his 1997 text.

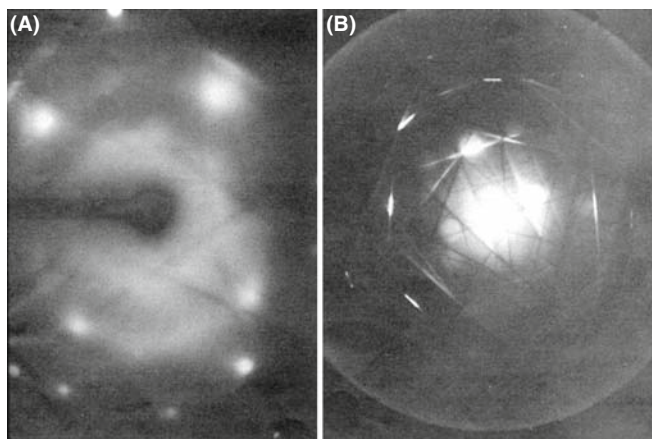


**FIGURE 20.13.** (A) Comparison of the poor quality of Kikuchi lines in an SADP and (B) the relatively clear distribution in a CBED pattern from deformed copper.

The generation of Kikuchi lines in a CBED pattern is marginally more complex than in an SADP. Remember how Kikuchi lines arise in a specimen illuminated by a parallel beam (see Chapter 19) and how a divergent beam of scattered electrons samples the various crystal planes (see Figure 20.14A). In Figure 20.14B you can see what happens when a convergent beam is used. In this case the incident rather than the scattered electrons span an angular range and therefore, just as in Kikuchi-line generation, some electrons in the beam will probably be at the exact Bragg angle to a ZOLZ plane (this is identical to the argument we used to explain the Kikuchi lines in LACBED patterns back in Figure 20.8A). Thus, there will be an elastic-scattering contribution to the Kikuchi lines where they cross the ZOLZ disks in CBED patterns. If you choose Kossel conditions (i.e.,  $2\alpha > 2\theta_B$ ) as in Figure 20.3F, there will *always* be electrons in the beam with the correct trajectory for exact Bragg diffraction from the planes in the *UVW* zone and so there will *invariably* be an elastic contribution to the Kikuchi lines.

Strictly speaking, we should only use the term ‘Kikuchi lines’ when inelastic scattering alone is responsible for their formation (i.e., the lines *between* any *hkl* disks). However, the term is used rather loosely in the literature to describe the ZOLZ intensity bands, despite the elastic contribution to the scattered intensity. Morniroli has proposed that this uncertainty be resolved by using the term ‘Bragg lines’ for the deficiency lines in CBED and LACBED patterns; this terminology is gaining wider acceptance.

## 20.8 HOLZ LINES

### 20.8.A The Relationship Between HOLZ Lines and Kikuchi Lines

As we just noted, Kikuchi lines can also arise from inelastic scattering by the HOLZ planes and HOLZ Kikuchi lines exist in many CBED patterns. You can see the array of deficient HOLZ Kikuchi lines between the ZOLZ maxima in Figure 20.2B. These HOLZ Kikuchi lines are, in principle, more useful than ZOLZ Kikuchi lines because they come from planes with much larger Bragg angles (and *g* vectors) so they are even more sensitive to changes in lattice parameter than the ZOLZ lines. Since

$$|\mathbf{g}| = \frac{1}{d}, |\Delta\mathbf{g}| = -\frac{\Delta d}{d^2} \quad (20.1)$$

then for smaller *d* values, the value of  $|\Delta\mathbf{g}|$  is much larger at the same  $\Delta d$ . We take advantage of this fact, not by using HOLZ Kikuchi lines specifically, but by seeking out a closely related phenomenon called HOLZ lines. HOLZ lines are simply the elastic part of the HOLZ Kikuchi lines, that is, they are the segments of the lines

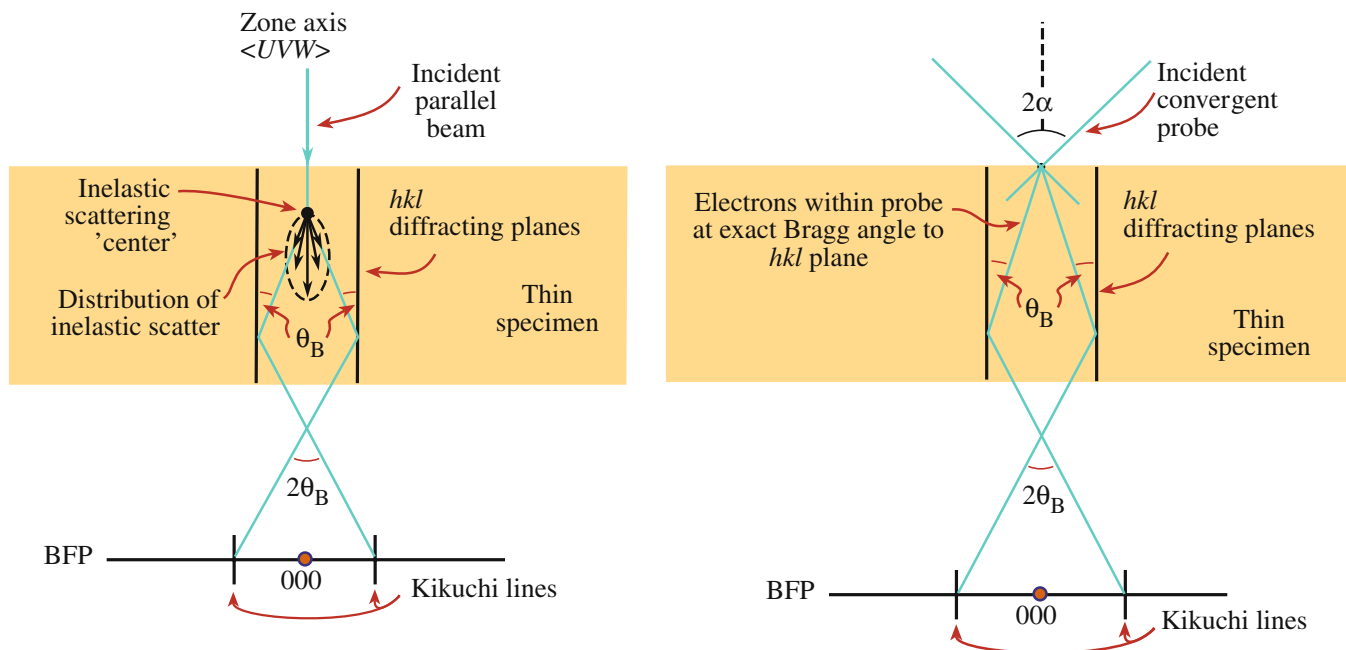


**FIGURE 20.14.** Comparison of the generation of Kikuchi lines (A) by inelastic scattering of electrons in a parallel beam and (B) by elastic scattering of electrons in a convergent beam when the convergence angle,  $\alpha$  is greater than the Bragg angle,  $\theta_B$ .

which appear *within* the diffraction maxima. By analogy with the production of Kikuchi lines and, as already shown in Figure 20.8A for LACBED patterns (although both these situations referred to ZOLZ diffraction), the HOLZ lines arise when electrons within the cone of the incident probe are at the correct Bragg angle for diffraction by a *HOLZ* plane. Therefore, these electrons are diffracted out to very high angles compared with ZOLZ diffraction. The result of this scattering is a bright line through the HOLZ disk and a dark line across the 000 disk. Not surprisingly, given what you've learned in the preceding nine chapters, the theory for the origin of HOLZ lines is much more complicated than this sparse summary. When you have time and the necessary inclination (tilt?) you should read the paper by Jones et al.

### PAIRS OF HOLZ LINES

HOLZ lines come in pairs, like Kikuchi lines, with the bright (excess) lines within the HOLZ *hkl* maxima and the dark (deficient) lines within the 000 disk.

An example of HOLZ lines is shown schematically in Figure 20.15, which compares with the experimental pattern in Figure 20.32B. Because these HOLZ lines contain 3D information they show the true, fcc, 3D, threefold  $\{111\}$  symmetry, while the ZOLZ Kikuchi lines and spots show sixfold, 2D,  $\{111\}$  symmetry. We will make use of

these differences when we discuss indexing such patterns and crystal-symmetry determination in Chapter 21 and in the companion text.

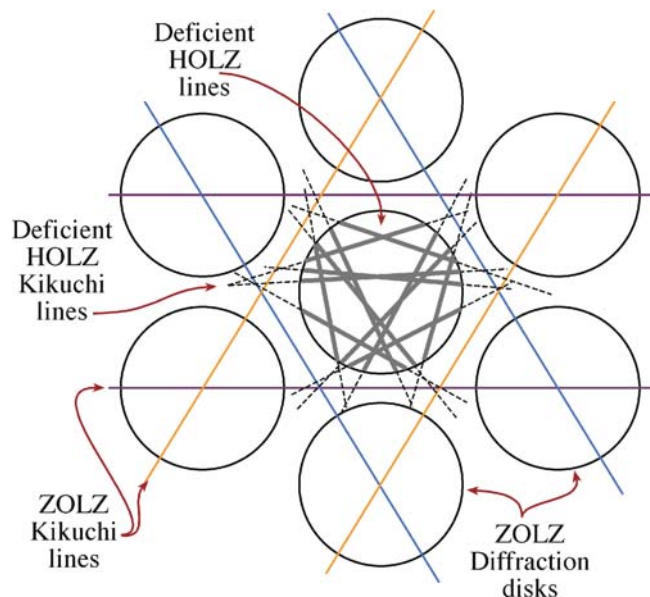


**FIGURE 20.15.** The relationship between Kikuchi lines and HOLZ lines is shown in this schematic of a  $\langle 111 \rangle$  CBED pattern from a cubic crystal. The three principal pairs of 220 ZOLZ Kikuchi bands show sixfold symmetry (characteristic of the 2D 111 planes) and bisect the  $\mathbf{g}$  vectors from 000 to the six 220 ZOLZ maxima. The *inelastic* deficient Kikuchi lines from the HOLZ planes are shown in the regions between the ZOLZ diffraction disks and the *elastic* deficient lines from the HOLZ planes are present within the 000 disk. In both cases, the HOLZ lines show threefold symmetry characteristic of looking down the  $\langle 111 \rangle$  direction in a 3D crystal.

## 20.8.B Acquiring HOLZ Lines

Steeds (1981) described the practical problems of recording HOLZ lines in some detail. Nothing much has changed in the intervening decades and the main points you have to consider are

- The lines are often only visible ‘on the negatives’ and not on the screen, so you should record all the DPs, not just ones on which you can see the lines. This poor visibility is less of a problem with a CCD because you can easily enhance the gain.
- You may have to make small changes in the operating voltage or the orientation in order to view the HOLZ rings, especially if the crystal has a small lattice-repeat spacing parallel to the beam and the angular view of the BFP is poor.
- Strains in the specimen from bending and thermal stresses smear out the HOLZ-line intensity. Choosing the smallest region (i.e., the smallest beam) may help this problem and will also minimize local thickness variations.
- Planar or point disorder as well as thermal (Debye-Waller) effects can reduce high-angle scattering. In practice, this means that cooling the specimen and reducing the kV can help to increase HOLZ-line visibility by reducing contamination and beam heating.
- Minor adjustments in HOLZ-line positions can help to distinguish HOLZ lines that overlap. To do this you need to change the kV by a small amount.

### CONTROLLING kV

Continuous kV control is an essential accessory to your TEM for serious CBED work.

The experimental procedure for observing HOLZ lines is quite straightforward but, since the lines themselves can be rather elusive, as we suggested at the start of the chapter, you should practice with a specimen such as Si or stainless steel in which the lines are almost always visible. The best way to search for the lines is

- Select the largest C2 aperture and go to the smallest  $L$  ( $\sim 3\text{--}500\text{ mm}$ ) at which you can see the full angular view of the BFP.
- Examine the Kossel/LACBED pattern (make  $2\alpha$  large) which should reveal Kikuchi bands intersecting at many poles, spanning a good fraction of the stereographic triangle as shown in Figure 20.16A.
- If you tilt to such a pole, as shown in Figure 20.16B, you should see the ring of HOLZ intensity.
- Tilt to a suitable zone axis for optimizing HOLZ effects. Remember, the best orientation for seeing the HOLZ lines in the 000 disk is *not* a low-index, high-symmetry pole such as  $\langle 100 \rangle$  or  $\langle 111 \rangle$ , but a higher-index, lower-symmetry one such as  $\langle 114 \rangle$ .
- To see the deficient lines, increase  $L$  to look in detail at the 000 region of the pattern, and if necessary, put in a

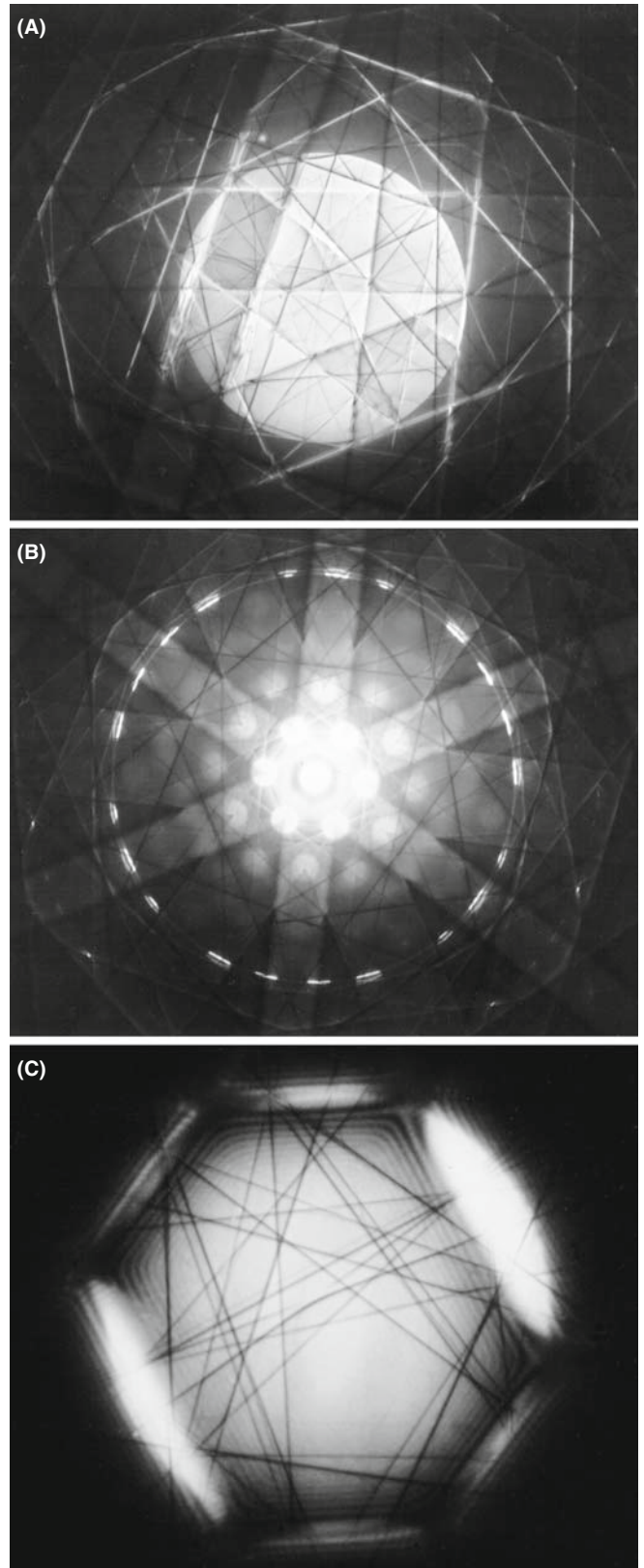


**FIGURE 20.16.** (A) Low- $L$ , large- $\alpha$  CBED pattern showing a wide area of reciprocal space, away from ZAP conditions. (B) When the specimen is tilted to a high-symmetry  $\langle 111 \rangle$  ZAP and a smaller C2 aperture is inserted, a ring of excess HOLZ lines appears. In (C) taken at high  $L$ , the deficient HOLZ lines are visible in the central 000 disk of the lower symmetry  $\langle 114 \rangle$  pattern.

smaller C2 aperture, center it and look for the fine dark lines crossing the bright disk as in Figure 20.16C. Usually, you'll just need this deficient-line distribution.

You have to use a range of  $L$  (from  $\sim 300$  to 1500 mm) to obtain all this information and this is easy in any post-1980 TEM. DSTEMs with sufficient post-specimen lenses are as versatile. Energy filtering improves everything that we've just described.

## 20.9 HOLLOW-CONE/PRECESSION CBED

As we described in Chapter 18, for SAD, we can acquire CBED patterns by rotating the incoming convergent beam about the optic axis in a hollow cone. Just as with SAD, hollow-cone CBED supplements the information we get in a stationary-beam pattern (i.e., all the patterns we've discussed so far). Remember, hollow-cone operation deflects the incident beam and rotates the pattern in the BFP while precession de-scans the beam so that the actual pattern is stationary. A good review of hollow-cone CBED and its relationship to other CBED methods is given in Tanaka's 1986 paper. Hollow-cone patterns do not show specific diffraction spots like CBED patterns since the rotating disk intensity is averaged out and the only stationary features are diffraction events at specific angles such as HOLZ lines. We can take advantage of this because if, for example, the cone angle is set to that of the FOLZ ring then the pattern consists predominantly of an array of excess HOLZ lines as shown in Figure 20.17. The ZOLZ disks, which would normally be so bright that they

might mask the excess lines, are removed because the rotation of the incident beam averages out the intensity.

Precession of CBED patterns has all the advantages of precession of SADPs as discussed in Section 18.8. A comparison of a precession DP and a standard DP under K-M conditions is shown in Figure 20.18. Precession extends the FOLZ ring into an annulus of width of  $\sim 10$  mrad. This dynamical background averaging can improve intensity measurements from DPs by considerably simplifying the problem of background subtraction.

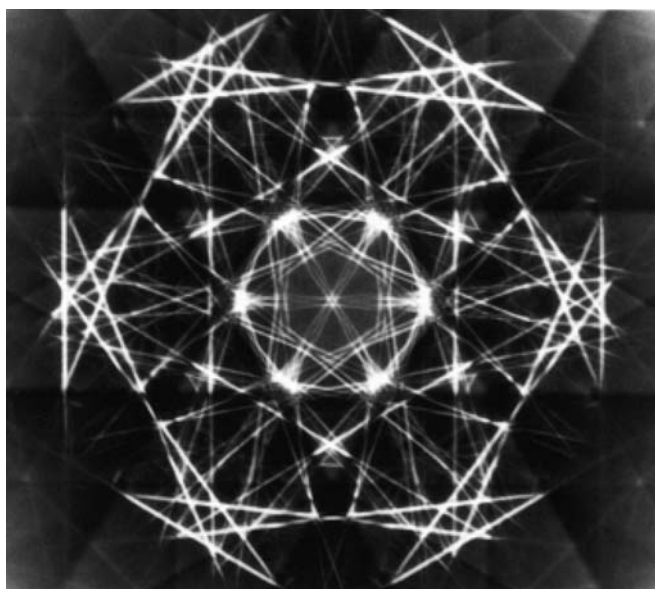


**FIGURE 20.17.** Hollow-cone CBED pattern showing bright, excess HOLZ lines only. All the usual diffraction-disk intensity is averaged out (Graphite 0001; 200 kV).

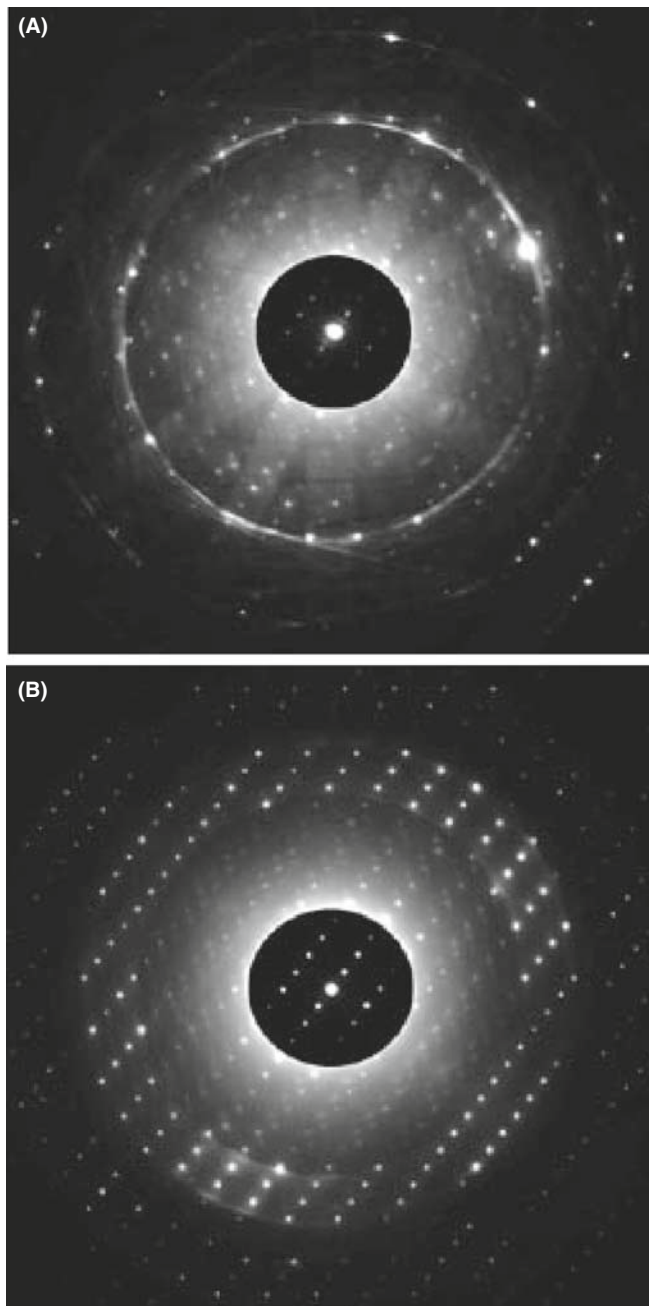


**FIGURE 20.18.** Comparison of (A) unprocessed and (B) precessed patterns from a very thick specimen of  $\text{Mg}_3\text{V}_2\text{O}_8$ . A small precession angle ( $\sim 5$  mrad) was used to form (B) and the reflections in the ZOLZ are more clearly defined. Dynamical scattering still contributes to the pattern so a thinner specimen would be better.

## CHAPTER SUMMARY

In this chapter we've covered how to obtain different CBED patterns experimentally. Particular points and terms that you should know are

- If you vary the specimen thickness,  $\alpha$ ,  $L$ , and the focus you can obtain CBED and LACBED patterns showing many different features. As with SAD, two-beam and zone-axis conditions are the standard operating conditions to get the most useful information.
- You'll probably have to record patterns at different values of  $\alpha$  and  $L$ , each with different exposure times.
- If you have an EELS then always filter your patterns.
- Even if you can filter the patterns, we strongly recommend using a double-tilt holder, cooled to LN<sub>2</sub> temperature.
- You must be able to change the kV by very small steps, if you are studying HOLZ lines.
- You can precess your CBED patterns or form them with hollow cones of incident electrons.
- Learn the meaning of such terms as ZAP, ZOLZ, FOLZ, HOLZ, K-M, and Kossel patterns.

In the next chapter, we'll show you how to use this contrast information to get the maximum amount of crystallographic information from your specimen.

### TEXTS

- Champness, PE 2001 *Electron Diffraction in the Transmission Electron Microscope* BIOS Oxford UK. A concise and essential summary textbook full of useful examples often from non-cubic systems, since the author is a mineralogist not a metallurgist.
- Morniroli, J-P 2002 *Large-Angle Convergent-Beam Electron Diffraction* SF $\mu$  (Société Française des Microscopies) Paris France. Highly recommended reading for serious students for whom CBED will be an important tool.
- Reimer, L (Ed.) 1995 *Energy-Filtering Transmission Electron Microscopy* Springer-Verlag New York. For some specifics.
- Reimer, L 1997 *Transmission Electron Microscopy; Physics of Image Formation and Microanalysis* (4th Ed.) Springer New York. For more specifics.
- Spence, JCH and Zuo, JM (Eds.) 1992 *Electron Microdiffraction* Kluwer New York. *The book for the dedicated CBED researcher.*
- Steeds, JW 1979 *Convergent Beam Electron Diffraction* in *Introduction to Analytical Electron Microscopy* 387–422 Eds. JJ Hren, JI Goldstein and DC Joy Plenum Press, New York. *The first book-chapter dedicated to the technique and still a superb introduction.*

### THE JEOL CBED ATLAS

This set of four volumes is perhaps the definitive work on CBED and describes an alternative approach to much of what is discussed in Chapters 20 and 21 and also in the companion text. The texts contain hundreds of beautiful and useful patterns.

- Tanaka, M and Terauchi, M 1985 *Convergent Beam Electron Diffraction* JEOL Tokyo.
- Tanaka, M, Terauchi, M and Kaneyama, T 1988 *Convergent Beam Electron Diffraction II* JEOL Tokyo.
- Tanaka, M, Terauchi, M and Tsuda, T 1994 *Convergent Beam Electron Diffraction III* JEOL Tokyo.
- Tanaka, M, Terauchi, M and Tsuda, T 2002 *Convergent Beam Electron Diffraction IV* JEOL Tokyo.

### HISTORY

Also see the references in Chapter 9.

- Kossel, W and Möllenstedt, G 1938 *Elektroneninterferenzen im konvergenten Bündel* Naturwissenschaften **26** 660–661.

### APPLICATIONS AND TECHNIQUES

- Heilmann, P, Clark, WAT and Rigney, DA 1983 *Orientation Determination of Subsurface Cells Generated by Sliding* Acta Met. **31**(8) 1293–1305.

- Humphreys, CJ, Maher, DM, Fraser, HL and Eaglesham, DJ 1988 *Convergent Beam Imaging – A Transmission Electron Microscopy Technique for Investigating Small Localized Distortions in Crystals* Phil. Mag. **58A** 787–798. CBIM.
- Jones, PM, Rackham, GM and Steeds, JW 1977 *Higher Order Laue Zone Effects in Electron Diffraction and Their Use in Lattice Parameter Determination* Proc. Roy. Soc. **A354** 197–222. When you have the time to really study HOLZ lines.
- Steeds, JW 1981 *Microanalysis by Convergent Beam Electron Diffraction in Quantitative Microanalysis with High Spatial Resolution* 210–216 Eds. GW Lorimer, MH Jacobs and P Doig The Metals Society London. For the terminology in Section 20.3.A.
- Tanaka, M, Saito, R, Ueno, K and Harada, Y 1980 *Large Angle CBED* J. Electr. Microsc. **29** 408–412.
- Tanaka, M 1986 *Conventional Transmission-Electron-Microscopy Techniques in Convergent-Beam Electron Diffraction* J. Electr. Microsc. **35** 314–323. Includes a good review of hollow-cone CBED.
- Wu, L, Zhu, Y and Taftø, J 1999 *Towards Quantitative Measurements of Charge Transfer in Complex Crystals Using Imaging and Diffraction of Fast Electrons* Micron **30** 357–369.

## APPLICATIONS AND TECHNIQUE

The companion text has a complete chapter devoted to CBED. Some of that material was in the original edition; it includes techniques that are still very powerful but that are not so widely used.

## SELF-ASSESSMENT QUESTIONS

- Q20.1 If CBED was invented before SAD, why did it only come into widespread use many years later?
- Q20.2 What advantages accrue when using a convergent rather than a parallel beam of electrons to create a diffraction pattern?
- Q20.3 What disadvantages are there to using CBED rather than SAD?
- Q20.4 How do you control the beam size in CBED?
- Q20.5 What are the advantages and disadvantages of using smaller beams to form CBED patterns?
- Q20.6 How do you control the size of the disks in the CBED pattern?
- Q20.7 Why would you want to change the camera length when viewing a CBED pattern?
- Q20.8 Define HOLZ, ZOLZ, FOLZ, K-M, ZAP, LACBED. Find any other acronyms from this chapter that are not in this list and define them.
- Q20.9 Explain why there is image information inside a CBED pattern disk when the pattern is not focused.
- Q20.10 Explain why this image effectively expands to infinite magnification when the pattern is focused.
- Q20.11 Why is it so important to align the C2 aperture when performing CBED?
- Q20.12 What is the role of thickness in CBED-pattern contrast?
- Q20.13 How can 3D information find its way into a 2D CBED pattern?
- Q20.14 Why is a higher-order ZAP preferable to a lower-order one for viewing a CBED pattern?
- Q20.15 Why do hollow-cone CBED patterns not show any diffraction disks, just HOLZ lines?
- Q20.16 What advantages accrue from precessing a CBED pattern?
- Q20.17 HOLZ lines within the 000 disk are continuous with lines outside this disk. What is the difference between the electrons contributing to the line within the disk and those in the line outside the disk?
- Q20.18 Why can we see Kikuchi lines in CBED patterns from specimens that are too thin to show such lines in SADPs or in specimens which are too deformed to show such lines in SADPs?
- Q20.19 Why do HOLZ lines appear more clearly at low temperatures?

## TEXT-SPECIFIC QUESTIONS

- T20.1 Look at Figure 20.1 and work out what would happen to the probe convergence angle if you switch on the C2 lens (a) weakly and (b) strongly enough to introduce a crossover before the upper objective lens. Sketch the ray diagrams for each case. Do the same for changing the size of the C2 aperture.
- T20.2 Look at the symmetry of the spots in Figure 20.2A and B and compare with the symmetry of the lines within the 000 disk in B. They are not the same. From what you know of the symmetry down the [111] direction in an fcc crystal, which pattern symmetry is correct? Why is the other symmetry observed?
- T20.3 Why does the intensity of the overall pattern increase from Figure 20.3D–F? Do you think the probe size has stayed constant as the C2 aperture has increased in size, and if not, why not? From what you know of lens limitations, what prevents us from keeping a very small probe size to localize the CBED pattern while increasing the current in the probe to generate a high-quality pattern? Are there experimental methods to overcome this problem?
- T20.4 Look at Figure 20.4 and explain why most of the intensity is in the 000 disk while it is barely possible to see the intensity scattered out to high angles in C. Is there anything you can do to increase the intensity scattered out to higher angles?

- T20.5 Draw schematic ray diagrams to explain the reversal in the image direction contained in the 000 disk in Figure 20.6 as the objective lens goes through focus.
- T20.6 List the pros and cons of forming CBED patterns in TEM versus STEM mode.
- T20.7 Why do you think that dynamical scattering causes regions of low (or zero) intensity to occur in CBED disks as in Figure 20.5B?
- T20.8 Explain what will happen to your CBED HOLZ intensity as you go to higher kVs. (Hint: look at Figure 20.11 and remember the effect of kV on  $\lambda$ .)
- T20.9 Compare and contrast HOLZ lines and Kikuchi lines in terms of their generation, intensity and distribution in low camera-length CBED patterns.
- T20.10 Since we know that the intensity of elastic scatter decreases rapidly with increasing angle away from the direct beam, where does the high intensity come from in the outer ring in Figure 20.16B?
- T20.11 Look at Figure 20.15. Explain what happens as the deficient HOLZ Kikuchi lines are extended such that they intercept other  $hkl$  disks in the ZOLZ.
- T20.12 Explain, with reference to Figure 20.8A, why it doesn't matter if you raise or lower the specimen out of the eucentric plane when forming a LACBED pattern. What experimental operation becomes increasingly difficult when you remove the specimen from the eucentric plane?
- T20.13 Why is the LACBED BF pattern so extensive while a LACBED DF pattern covers only a very small region of reciprocal space (e.g., see Figure 20.9)?